

Glueballs on the three-sphere

Bas van den Heuvel

Instituut-Lorentz for Theoretical Physics,
University of Leiden, P.O. Box 9506,
NL-2300 RA Leiden, The Netherlands.

Abstract: We study the non-perturbative effects of the global features of the configuration space for $SU(2)$ gauge theory on the three-sphere. The strategy is to reduce the full problem to an effective theory for the dynamics of the low-energy modes. By explicitly integrating out the high-energy modes, the one-loop correction to the effective hamiltonian is obtained. Imposing the dependence through boundary conditions in configuration space incorporates the non-perturbative effects of the non-contractable loops in the full configuration space. After this we obtain the glueball spectrum of the effective theory with a variational method.

1 Introduction

One of the methods to gain understanding of non-perturbative phenomena in non-abelian gauge theory is by using the finite-volume approach [1, 2]. The mechanism of asymptotic freedom [3] renders the coupling constant small at high energies or, equivalently, at small distances. Taking the finite volume to be small results in a small coupling constant: one can use perturbation theory. Gradually increasing the volume then allows one to study the onset of non-perturbative phenomena and to see, hopefully, the setting in of confinement. In this regime one can employ a hamiltonian formulation [4] of the problem. The strategy in studying the dynamics of the Yang-Mills field is based on two observations. First, quantum field theory can in a sense be regarded as ordinary quantum mechanics, but with an infinite number of degrees of freedom. For the case of non-abelian gauge field theory, the configuration space of this quantum mechanical problem is complicated, which gives rise to non-perturbative behaviour. Second, coming from the perturbative regime, these complications first show up in the low-energy modes of the gauge field: one can capture the influence of the topology of the configuration space by studying the effective theory of the finite number of affected modes.

Let us first reformulate quantum field theory as quantum mechanics. In the hamiltonian picture we are dealing with wave functionals in the configuration space. Speaking generally, each point in the configuration space corresponds to a configuration of the fields $\phi(\mathbf{x})$. This means we have fields $\phi(\mathbf{x})$, conjugated momenta $\pi(\mathbf{x})$, a hamiltonian $H[\pi; \phi]$ and

wave functionals $|\Psi\rangle$. If we decompose the fields $\phi(x)$ in orthogonal modes, we can reformulate the hamiltonian problem in terms of the generalized Fourier coefficients q_k and their conjugate momenta p_k . This leads to a hamiltonian $H[q_k; p_k]$ and wave functionals $|\Psi[q_k]\rangle$. A typical hamiltonian would look like

$$H[q_k; p_k] = \sum_k \left(p_k^2 + \frac{1}{2} q_k^2 \right) + \text{interaction terms} \quad (1)$$

At small coupling, the modes will not interact and the potential will rise quadratically in all directions. As a consequence, the wave functions will be the familiar harmonic oscillator wave functions. One subsequently uses perturbation theory to take the interactions between this infinity of modes into account. What we have just described is the ordinary perturbative approach to quantum field theory. This perturbation scheme breaks down when at larger coupling the behaviour of the wave function for some of the modes is dictated by the properties of the configuration space, as explained below. We then have to replace these wave functions by functions that have the behaviour required by the configuration space. In this regime the hamiltonian method is superior to the covariant path integral approach of Feynman.

An essential feature of the non-perturbative behaviour is that the wave functional spreads out and becomes sensitive to the global features of the configuration space. This spreading out of the wave functional will occur first in those directions of the configuration space where the potential energy is lowest, i.e. in the direction of the low-energy modes of the gauge field (small q_k). If the configuration space has non-contractable circles, the wave functionals are drastically affected by the topology when the support of the wave functional extends over the entire circle (i.e. bites in its own tail). This is what typically happens in non-abelian gauge theories. The Yang-Mills configuration space is the space of gauge orbits A/G (A is the collection of gauge fields or connections, G the group of local gauge transformations). We know from Singer [5] that the topology of this configuration space is highly non-trivial when G is non-abelian. The configuration space also has a Riemannian geometry [6] that can be made explicit, once explicit coordinates are chosen on A/G . This geometry also influences the wave functionals, if the latter are no longer localized within regions much smaller than the inverse curvature of the field space.

One of the most prominent properties of a non-abelian gauge theory, is the multiple vacuum structure. This means that the gauge degrees of freedom cannot be completely removed [7] by imposing a simple condition like the Coulomb gauge. After gauge fixing there will remain Gribov copies, that is, gauge equivalent gauge field configurations that all satisfy the gauge fixing condition. Intimately related to this is the existence of instantons [8]. They can be shown to describe tunnelling between gauge copies of the vacuum, that is, tunnelling from one Gribov copy to another. The configuration sitting at the top of the tunnelling path with lowest energy barrier is called the sphaleron [9]: it is a saddle-point of the potential with one unstable mode. Let us suppose that, coming from the vacuum, the potential energy in the direction of the sphaleron(s) grows slowly. This means that at increasing volume the wave functionals around the different gauge copies of the vacuum will start to flow out over the instanton barriers and will develop a substantial overlap with each other. We then have the situation described above of probing the non-contractable loops in configuration space.

We impose gauge invariance by restricting the dynamics to a fundamental domain, that is, a set of gauge fields that is in one-to-one correspondence with the physical configuration space $A = G/[10, 11, 12]$. Explicitly, we first define \mathcal{A}^0 to be the set of gauge field configurations A with the property that $gA = A$ for all gauge transformations g . We will take this gauge field to represent the orbit on which it lies. One shows that \mathcal{A}^0 is a convex subset of the set of transverse gauge fields, and that $\mathcal{A}^0 \neq \emptyset$, where \mathcal{A} is the Gribov region which is characterized by the condition that the Faddeev-Popov operator is positive: $\text{FP}(A) > 0$. As \mathcal{A}^0 is a convex subset of a linear vector space, it is topologically trivial. In order to get a one-to-one correspondence between \mathcal{A}^0 and $A = G$, certain points on the boundary of \mathcal{A}^0 (these are the points where the minimum of the norm of the gauge field on the orbit is degenerate) must be identified, after which we denote \mathcal{A}^0 by \mathcal{A} . Only after these boundary identifications, \mathcal{A} has the non-trivial topological structure of the physical configuration space. If we restrict the dynamics to the fundamental domain \mathcal{A} , the boundary identifications give rise to boundary conditions on the wave functional. See fig.1 to get an idea of how the potential landscape might look in relation to the various spaces defined above. This figure displays a two-dimensional subspace (consisting of low-energy modes) of the configuration space.

The use of the hamiltonian formulation is especially fruitful when the non-perturbative effects manifest themselves appreciably only in a small number of the modes of the gauge field. For this limited number of modes one defines an effective hamiltonian that takes the perturbative effect of all the other modes into account [1]. By studying the resulting ordinary quantum mechanical problem, one can go beyond purely perturbative results [2].

Apart from offering the possibility to go beyond perturbation theory, the finite-volume approach sketched above, which is sometimes called 'analytical', has the merit of being directly comparable to the numerical results of lattice calculations. For this the finite volume of the analytic approach must be chosen to be the finite volume of the lattice calculations. Putting a theory on a finite lattice necessarily means that it is put in a finite volume with certain boundary conditions. For the standard lattice geometry, this finite volume is cubic with periodic boundary conditions, i.e. a torus.

To make the reduction of an infinite to a finite number of degrees of freedom, we use the Born-Oppenheimer approximation, which has its origin in the quantum mechanical treatment of molecules. In field theory one integrates out the fast modes from the path integral and obtains an effective hamiltonian in a finite number of slow modes. Using these methods in the intermediate-volume regime for $SU(2)$ gauge theory on the torus resulted in good agreement with the lattice results [2, 13]. In case of periodic boundary conditions on the torus and already at small volumes, one should take into account non-perturbative effects in the effective theory due to tunnelling through quantum induced barriers. These barriers are contributions to the potential coming from the integrating out of the fast modes. This tunnelling sets in much before the instanton effects play any role. Koller & Van Baal [2] have shown that one can derive very accurate results, beyond the semiclassical analysis, by imposing non-trivial boundary conditions on the wave functional at the corresponding sphalerons.

However one would like to extend these results to larger volumes in an attempt to get as close as possible to the continuum domain, and in this way get some intuition about how continuum sets in. The first thing to do, as argued above, is to include contributions

coming from instantons: one wants to take into account the sphaleron directions in configuration space, because there the potential will show the strongest deviation from gaussian behaviour. This is not an easy task first of all because the instanton solutions on a torus are only known numerically [14].

To avoid this problem, we have shifted our attention to the case where the finite volume is S^3 , (the surface of) a three-sphere [15]. Here the instantons are known analytically, and the tunnelling paths that connect gauge copies of the vacuum lie within the space of low-energy modes. Another simplification is that the structure of the perturbative vacuum is much simpler than in the case of the torus: there is no vacuum valley, that is, there is no continuous set of minima of the classical potential. A drawback of the three-sphere is that we lose the possibility to check against lattice results. Also, the approach to infinite-volume results will go as powers of $1/R$ as compared to the exponential behaviour in L for the torus [16]. Thus, due to the intrinsic curvature of S^3 , it will be even less easy to derive infinite-volume results from our calculations. Nevertheless, within this model one can study non-perturbative phenomena like the effects of large gauge transformations and especially of the θ angle on the glueball spectrum. A gauge transformation is called ‘large’ if it cannot be continuously deformed into the identity. Typically, two Gribov copies of the vacuum are related by a large gauge transformation. The θ angle, which will be properly defined in section 2, is a free parameter of the theory that one has to allow when one implements gauge invariance under large gauge transformations. The conditions at the boundary of the fundamental domain will depend on the θ angle, thus incorporating the non-perturbative effects of the non-contractable loops in the full configuration space. Previous research into gauge theory on S^3 [17] did not include the study of the effects of large gauge transformations.

This paper is set up as follows. In section 2 we define the effective model. In section 3 we explicitly integrate out the high-energy modes using a background field method [18]. This gives us the one-loop correction to the effective potential. In section 4 we construct a basis of functions that respect the (θ -dependent) boundary conditions. Using this basis we perform a Rayleigh-Ritz analysis to approximate the spectra of both the lowest order hamiltonian and of the one-loop corrected hamiltonian. Summaries of these results appeared in respectively [19] and [18]. From the eigenvalues one can obtain the masses of the different excitations (the glueballs) in this model. Section 5 contains a discussion of the results. We argue that the effect of the instantons is large, but calculable. We determine the range of validity of the effective model and show that the results are in reasonable agreement with results on the torus.

2 The effective model

2.1 Introduction

In this section we will define the effective model. First, the necessary machinery needed for the analysis on S^3 is developed. In particular, we will write down bases of functions for scalar and vector functions on S^3 . These bases of functions will be used in section 3 for the evaluation of various functional determinants. These functions will also allow us to isolate the space of low-energy modes on which the effective theory will be defined. After this we

will familiarize ourselves with some of the topological properties of $SU(2)$ gauge theory on the three-sphere and we show how the instanton degrees of freedom are embedded in the space of slow modes. Then we will describe the derivation of the effective hamiltonian, and discuss the validity of the adiabatic approximation. The hamiltonian itself need to be supplemented with suitable boundary conditions in field space to obtain a well-posed quantum mechanical problem. These conditions emerge when imposing gauge invariance through restricting our problem to the fundamental domain. We will use dynamical considerations to argue that we have enough freedom to choose tractable boundary conditions.

2.2 Low-energy modes

We begin by introducing two framings on S^3 . These will lead to a basis of scalar functions. By taking tensor products of these scalar modes with eigenfunctions of the spin operator, we will construct vector functions on S^3 . By a similar method we will also construct $su(2)$ -valued functions, where $su(2)$ denotes the Lie algebra corresponding to the Lie group $SU(2)$. After this we will write down the space of low-energy modes for $SU(2)$ gauge theory on S^3 .

Let σ_a be the Pauli matrices. We introduce the unit quaternions and their conjugates σ^{\pm} by

$$\sigma^+ = (\mathbb{1}; i\sigma^3); \quad \sigma^- = (\mathbb{1}; -i\sigma^3); \quad (2)$$

They satisfy the multiplication rules

$$\sigma^+ \sigma^+ = 0; \quad \sigma^- \sigma^- = 0; \quad (3)$$

where we used the 't Hooft symbols [20], generalized slightly to include a component symmetric in i and j for $\sigma^{\pm} = 0$. The σ^{\pm} and σ^{\pm} form bases for respectively the self-dual and anti-self-dual four by four matrices. The symbols enjoy the following useful relations

$$\sigma^+ \sigma^+ = 0; \quad \sigma^- \sigma^- = 0; \quad \sigma^+ \sigma^- = \sigma^- \sigma^+ = \mathbb{1}; \quad (4)$$

We can use σ^{\pm} and σ^{\pm} to define orthonormal framings of S^3 , which were motivated by the particularly simple form of the instanton vector potentials in these framings (see section 2.3). We embed S^3 in R^4 by considering the unit sphere parametrized by a unit vector n . Using the scale-invariance of the classical hamiltonian, we can make the restriction to a sphere of radius $R = 1$. The R dependence can be reinstated on dimensional grounds. The framing for S^3 is obtained from the framing of R^4 by restricting in the following equation the four-index ϵ to a three-index a (for $\sigma^{\pm} = 0$ one obtains the normal n on S^3):

$$e^+ = \epsilon^{+abc} n^a; \quad e^- = \epsilon^{-abc} n^a; \quad (5)$$

The orthogonal matrix V that relates these two frames is given by

$$V_j^i = e^i e^j = \frac{1}{2} \text{tr}((n^i n^j)_{ij}): \quad (6)$$

Note that e and e have opposite orientations. The parity operation P defined by

$$P : (n_0; \mathbf{n}) \rightarrow (n_0; -\mathbf{n}); \quad (7)$$

interchanges the e and the e framing.

A vector field A can be written with respect to either framing (5). From now on we will, unless stated otherwise, use the framing e^i and write

$$A = A_i e^i : \quad (8)$$

Since we want vector fields to be tangent to S^3 we have that $n \cdot A = 0$ and the sum over i runs from 1 to 3. Latin indices refer to this framing, while Greek indices will refer to the embedding space \mathbb{R}^4 .

Each of the framings (5) defines a differential operator

$$\partial^i = e^i \frac{\partial}{\partial x}; \quad \partial^i = e^i \frac{\partial}{\partial x}; \quad (9)$$

to which belong $\mathfrak{su}(2)$ angular momentum operators, which for historical reasons will be denoted by \tilde{L}_1 and \tilde{L}_2 :

$$L_1^i = \frac{i}{2} \partial^i; \quad L_2^i = \frac{i}{2} \partial^i : \quad (10)$$

They are easily seen to commute and to satisfy the condition

$$\tilde{L}^2 - \tilde{L}_1^2 = \tilde{L}_2^2 : \quad (11)$$

The manifold S^3 is isomorphic to the Lie group $SU(2)$. The spatial symmetries of S^3 correspond to the left and right action of $SU(2)$ on itself: $\mathfrak{so}(4) = \mathfrak{su}(2) \oplus \mathfrak{su}(2)$. In appendix A we show that \tilde{L}_1 and \tilde{L}_2 correspond to the generators of the left and right symmetries on $SU(2)$.

A basis of scalar functions on S^3 is given by the set of eigenfunctions of the commuting operators $\tilde{L}^2; L_{1z}; L_{2z}g$:

$$j|l m_L m_R i; \quad l = 0; \frac{1}{2}; 1; \dots; \quad m_L; m_R = -l; \dots; l : \quad (12)$$

Since the Laplacian on S^3 is given by $\partial_i \partial_i = -4\tilde{L}^2$, these modes are eigenfunctions of the spherical Laplacian with eigenvalue $-4l(l+1)$ and degeneracy $(2l+1)^2$. See appendix A for other ways to arrive at this basis.

To classify vector fields A_i on S^3 , we introduce a spin operator S by $(S^a A)_i = i \epsilon_{aij} A_j$. This is an $\mathfrak{su}(2)$ angular momentum operator that commutes with \tilde{L}_1 and \tilde{L}_2 . We also define $K = \tilde{L} + S$, which is shorthand for $K_{ij} = \tilde{L}_{ij} + S_{ij}$. When there is no confusion possible, we will write \tilde{L} for \tilde{L}_1 . The fact that we single out \tilde{L}_1 is related to the fact that we chose e^i as the preferred framing for expressing vector fields. A basis of vector fields can be obtained by taking tensor products of the scalar functions (12) with the basis functions $j|l m_S i$ of the spin operator. In the standard way one obtains eigenfunctions of the set $fK; \tilde{L}_2 g$:

$$j|l m_R; k m_K i; \quad l = 0; \frac{1}{2}; 1; \dots; \quad k = j-1; j; \dots; j+1 : \quad (13)$$

The three modes with $(l; k) = (0; 1)$ are the three vector fields e^i . The three vector fields $e^j = V_i^j e^i$ correspond to the modes with $(l; k) = (1; 0)$, as can be seen from $L_1^k V_i^j = i \epsilon_{kim} V_m^j$. To identify transversal and longitudinal modes, first note that $\partial \cdot A = \partial_i A_i$. Next

we introduce the operator Q via $Q_{ij} = L_i L_j$. Note that $QA = 0$ for A in the Coulomb gauge. Using the identity

$$L^2 S^2 = L^2 - L \cdot S \cdot Q; \quad (14)$$

one concludes that the modes with $k = l - 1$ are transverse, whereas the modes with $k = l$ are purely longitudinal.

To deal with $su(2)$ -valued functions, we introduce the isospin operator T by $T^a = \text{ad}(\frac{1}{2} \tau^a)$, where $\text{ad}(X)(Y) = [X, Y]$. This operator is yet another $su(2)$ angular momentum operator that commutes with all operators defined before. By taking tensor products of the functions obtained so far with the basis functions jlm of T , we can construct scalar and vector modes that take their values in $su(2)$. Introducing $J = L + T$ we obtain for the $su(2)$ -valued scalar functions (e.g. in infinitesimal gauge transformations on S^3)

$$jlm_R; jm_j i; \quad l = 0; \frac{1}{2}; 1; \dots; \quad j = j_l - 1; j; \dots; l + 1; \quad (15)$$

For the vector functions (e.g. gauge fields on S^3) we define $J = K + T$ and obtain

$$jlm_R; k; jm_j i; \quad l = 0; \frac{1}{2}; 1; \dots; \quad k = j_l - 1; j; \dots; l + 1; \\ j = j_k - 1; j; \dots; k + 1; \quad (16)$$

Generalizing to the case where S and T correspond to respectively a spin- s and a spin- t representation, we obtain (suppressing the m_R dependence)

$$j; (ls)k; jm_j i; \quad l = 0; \frac{1}{2}; 1; \dots; \quad k = j_l - s; j; \dots; l + s; \\ j = j_k - t; j; \dots; k + t; \quad (17)$$

The scalar modes are recovered by the choice $s = 0, t = 1$, the vector modes correspond to the choice $s = 1, t = 1$.

An $SU(2)$ gauge field on the three-sphere can be written as

$$A = A_i e^i = A_i^a e^i \frac{\tau^a}{2}; \quad (18)$$

The field strength is given by $F_{ij} = \partial_i A_j - \partial_j A_i + [A_i, A_j] - 2\epsilon_{ijk} A_k$, where the last term is the so-called spin-connection: it is a consequence of the fact that we used a framing on the curved manifold S^3 . Reinstating the radius R would lead to a factor $1/R$ for this last term, which shows that this term vanishes in the limit of no curvature, i.e. for $R \rightarrow \infty$. A gauge transformation $g: S^3 \rightarrow SU(2)$ acts as follows:

$$(A)_i = g^{-1} A_i g + g^{-1} \partial_i g = g^{-1} D_i(A) g; \quad (19)$$

where $D(A)$ denotes the covariant derivative in the fundamental representation. As usual, the field strength F transforms under the adjoint representation: $(F)_{ij} = g^{-1} F_{ij} g$. In order to isolate the lowest energy levels, we examine the potential energy

$$V(A) = \frac{1}{2} \int_{S^3} \text{tr}(F_{ij}^2); \quad (20)$$

Note the factor 2^{-2} that we absorbed in the potential. We define the quadratic fluctuation operator M by

$$V(A) = \frac{1}{2^{-2}} \int_{S^3} \text{tr}(A_i M_{ij} A_j) + O(A^3) : \quad (21)$$

This gives

$$M_{ij} = 2L_{ij}^2 + 2K_{ij}^2 - 4Q_{ij} : \quad (22)$$

Using $S^2 = 2$ and eq. (14) one rewrites

$$M_{ij} = K^2 - L_{ij}^2 : \quad (23)$$

Now focus on the modes (16). For $l=0$, we have $k=1$ and $M=4$. The 9 eigenmodes are $A_i^a = c_1^a$ with c_1^a constant. For $l=\frac{1}{2}$, the modes with $k=\frac{1}{2}$ are pure gauge ($M=0$ and $Q \neq 0$), whereas the modes with $k=\frac{3}{2}$ are physical with $M=9$. For $l=1$, the modes with $k=1-1$ have $M=(2l)^2$, the modes with $k=1+1$ have $M=(2(l+1))^2$ and the modes with $k=1$ are again pure gauge. In particular the 9 modes with $l=1; k=0$ have $M=4$ and are given by $A_i^a = d_m^a V_i^m$ with d_m^a constant. The lowest eigenspace of M is thus 18 dimensional and given by

$$A(c;d) = c_i^a + d_j^a V_i^j e^i \frac{a}{2} = c_i^a e^i + d_j^a e^j \frac{a}{2} : \quad (24)$$

This is the space on which we will build the effective theory.

2.3 Winding numbers and instantons

Before writing down the instantons, we first introduce the notions of winding number and topological charge. The reader is referred to [21] for more details.

In the $A_0 = 0$ gauge, the set of gauge transformations G consists of mappings $g : S^3 \rightarrow SU(2) = S^3$. As a consequence, G splits up in distinct classes that can be labelled by the winding number of the gauge transformations in that class:

$$n[g] = \frac{1}{24^{-2}} \int_{S^3} \epsilon_{ijk} \text{tr} (g^{-1} \partial_i g) (g^{-1} \partial_j g) (g^{-1} \partial_k g) : \quad (25)$$

Gauge transformations with zero winding number can be continuously deformed into the identity mapping, whereas mappings with non-zero winding number cannot. The latter mappings are sometimes referred to as 'large' or 'homotopically non-trivial' gauge transformations.

Related to this, we define the standard Chern-Simons functional that measures the topological charge of a gauge field configuration:

$$Q[A] = \frac{1}{16^{-2}} \int_{S^3} \epsilon_{ijk} \text{tr} A_i F_{jk} - \frac{2}{3} A_i A_j A_k : \quad (26)$$

The sign of $n[g]$ was chosen such that we have $Q[A] = Q[A] + n[g]$.

In the hamiltonian picture, gauge invariance is implemented through Gauss' law, which implies invariance of the wave functional under small gauge transformations. For large gauge transformations, we have to allow for a possible angle:

$$[A] = e^{in[g]} [A]: \quad (27)$$

The (anti-)instantons [8] in the framings (5), obtained from those on R^4 by interpreting the radius in R^4 as the exponential of the time in the geometry $S^3 \times R$, become e^u and $e^{\bar{u}}$ are defined with respect to the framing e^a for instantons and with respect to the framing $e^{\bar{a}}$ for anti-instantons)

$$A_0 = \frac{u}{2(1 + |u|^2)}; \quad A_a = \frac{\bar{u} \wedge u}{2(1 + |u|^2)}; \quad (28)$$

where

$$u = \frac{2s^2}{1 + b^2 + s^2}; \quad \bar{u} = \frac{2sb}{1 + b^2 + s^2}; \quad s = e^t; \quad (29)$$

The instanton describes tunnelling from $A = 0$ ($Q=0$) at $t = -1$ to $A_a = \frac{a}{2}$ ($Q=1$) at $t = 1$, over a potential barrier that is lowest when $b = 0$. This configuration (with $b = 0, u = 1$) corresponds to a sphaleron [9], i.e. the vector potential $A_a = \frac{a}{2}$ is a saddle point of the energy functional with one unstable mode, corresponding to the direction (u) of tunnelling. At $t = 1$, $A_a = \frac{a}{2}$ has zero energy and is a gauge copy of $A_a = 0$ by a gauge transformation $g = n$ with winding number one, since

$$n \cdot \partial_n = a: \quad (30)$$

We will be concentrating our attention to the c and d modes of eq. (24). These modes are degenerate in energy to lowest order with the modes that describe tunnelling through the sphaleron and "anti-sphaleron". The latter corresponds to the configuration with the minimal barrier height separating $A = 0$ from its gauge copy by a gauge transformation $g = n$ with winding number -1 . The anti-sphaleron is actually a copy of the sphaleron under this gauge transformation, as can be seen from eq. (28), since

$$n \cdot \partial_{\bar{a}n} = \bar{a}: \quad (31)$$

The two-dimensional space containing the tunnelling paths through the sphalerons is consequently parametrized by u and v through

$$A(u;v) = ue^a - ve^{\bar{a}} - \frac{a}{2} = A_i(u;v)e^i; \quad (32)$$

$$A_i(u;v) = (u \frac{a}{2} - v \frac{\bar{a}}{2}) \frac{a}{2} = u \frac{1}{2} + v n - \frac{1}{2} n: \quad (33)$$

The gauge transformation with winding number -1 is easily seen to map $(u;v) = (w;0)$ into $(u;v) = (0;2-w)$. In particular, as discussed above, it maps the sphaleron $(1;0)$ to the anti-sphaleron $(0;1)$. Comparing with eq. (24) shows that we obtain the $(u;v)$ space from the $(c;d)$ space by the choice $c_i^a = u \frac{a}{2}$ and $d_i^a = v \frac{\bar{a}}{2}$.

2.4 Reduction to a quantum mechanical problem

Let us start with the naive derivation of the hamiltonian for the (c;d) modes. From the lagrangian

$$L = \frac{1}{4g^2} \int_{S^3} F^a F^a = \frac{1}{2g^2} \int_{S^3} F_{0i}^a F_{0i}^a - \frac{2}{g^2} V(A); \quad (34)$$

we obtain for the (c;d) space

$$L = \frac{2}{2g^2} \int_{S^3} \dot{c}_i^a \dot{c}_i^a + \dot{d}_i^a \dot{d}_i^a - \frac{2}{g^2} V(c;d); \quad (35)$$

This leads to the hamiltonian

$$H = \frac{f}{2} \left(\frac{\partial^2}{\partial c_i^a \partial c_i^a} + \frac{\partial^2}{\partial d_i^a \partial d_i^a} \right) + \frac{1}{f} V(c;d); \quad f = \frac{g^2}{2}; \quad (36)$$

where the potential $V(c;d) = V_{cl}(c;d)$ can be obtained from eq. (20):

$$V(c;d) = V(c) + V(d) + \frac{1}{3} (\text{tr}(X) \text{tr}(Y) - \text{tr}(XY)); \quad (37)$$

$$V(c) = 2 \text{tr}(X) + 6 \det c + \frac{1}{4} \text{tr}^2(X) - \text{tr}(X^2); \quad (38)$$

with the symmetric matrices $X = cc^T$ and $Y = dd^T$.

The correct way to obtain the effective hamiltonian for the (c;d) modes must start from the full theory. In the case where the finite volume is the three-torus all zero momentum states become degenerate with the ground state at $g = 0$. This infinite degeneracy allows one to derive an effective hamiltonian for these states using degenerate hamiltonian perturbation theory starting from the full hamiltonian \hat{H} [1]. This full hamiltonian in the Coulomb gauge is given in [4]. Proceeding to higher order in this way is complicated, mainly due to the non-abelian Coulomb Green function that occurs in the kinetic part of the hamiltonian, but it can be done [22].

For the case of the three-sphere however, the ground state at $g = 0$ is non-degenerate. The (c;d) modes are in this respect not the analogue of the zero momentum modes on the torus, but are singled out just because of the fact that they are the slow modes of the system. To calculate the effective hamiltonian for these modes, we compute the effective action for the (c;d) degrees of freedom using a background field method. This explicit calculation will be performed in section 3.

We will use the hamiltonian formulation of the full problem for the discussion of the validity of restricting ourselves to the (c;d) space. Let x denote the 18 (c;d) modes and q all the transverse modes orthogonal to the (c;d) space. We use p_x and p_q to denote the conjugate momenta. The full hamiltonian in the Coulomb gauge [4] is a function of x , p_x , q and p_q . We define

$$H_{[x]} = \hat{H}(x; p_x = 0; q; p_q); \quad (39)$$

Consider the following decomposition of the full wave function

$$= \sum_{n=1}^{\infty} \psi^{(n)}(x) \chi^{(n)}_{[x]}(q); \quad (40)$$

where the functions $\psi_i = \psi_i^{(n)}(\mathbf{q})$ are chosen to be eigenstates of $H_{[\mathbf{x}]}$:

$$H_{[\mathbf{x}]} \psi_i^{(n)}(\mathbf{q}) = V^{(n)}(\mathbf{x}) \psi_i^{(n)}(\mathbf{q}) : \quad (41)$$

The Schrodinger equation $\hat{H} \psi = E \psi$ is equivalent to the following set of equations:

$$\sum_{m=1}^{\infty} \langle \mathbf{x} | p_x; q; p_q \rangle \psi_m^{(n)}(\mathbf{x}) \psi_i^{(n)} = E \psi_i^{(n)}(\mathbf{x}) \quad \forall n : \quad (42)$$

As an example we assume the following form for the full hamiltonian,

$$\hat{H} = \frac{f}{2} \frac{\partial^2}{\partial x_1^2} + \frac{1}{f} V_{\text{cl}}(\mathbf{x}) + H_{[\mathbf{x}]}(q; p_q) : \quad (43)$$

This would be the form of the full hamiltonian if we neglect the complications of the non-abelian Coulomb Green function. The Schrodinger equation for this case leads to

$$\frac{f}{2} \frac{\partial^2}{\partial x_1^2} \psi_m^{(n)}(\mathbf{x}) + \left(\frac{1}{f} V_{\text{cl}}(\mathbf{x}) + V^{(n)}(\mathbf{x}) \right) \psi_i^{(n)}(\mathbf{x}) = E \psi_i^{(n)}(\mathbf{x}) \quad \forall n : \quad (44)$$

Here we introduced the covariant derivative r by

$$r_{nm}^i = \frac{\partial}{\partial x_i} \psi_{nm}^i + \langle \mathbf{x} | \frac{\partial}{\partial x_i} \psi_i = \frac{\partial}{\partial x_i} \psi_{nm}^i + A_{nm}^i : \quad (45)$$

The adiabatic approximation consists of truncating this equation to $\psi^{(1)}$, that is, we assume the transverse wave function to be in its ground state and we assume this ground state to decouple dynamically from the excited states. This approximation is valid if either the coefficients A_{nm}^i are small, or if we are in the region where the energy difference $V^{(2)}(\mathbf{x}) - V^{(1)}(\mathbf{x})$ is large compared to the excitation energies of the states we are interested in.

Returning to the general problem, the equations for the functions $\psi^{(n)}(\mathbf{x})$ will not just contain the functions A_{nm}^i defined above, but more general matrix elements of the form $\langle \mathbf{x} | p_x; q; p_q \rangle \psi_i^{(n)}$. Still, if the excitation energies are small compared to $V^{(2)}(\mathbf{x}) - V^{(1)}(\mathbf{x})$, the higher ψ 's will be small and we can restrict eq. (42) to $\psi^{(1)}$.

2.5 Boundary conditions

We impose gauge invariance by restricting the dynamics to the fundamental domain. The configuration space of our effective model consists of the intersection of with the space of low-energy modes, the $(c; d)$ space. This space was investigated in [12], and the information obtained there on the boundary of the fundamental domain will be sufficient for our present purposes. To see this focus on the two-dimensional $(u; v)$ plane (g1), which contains the tunnelling paths. We have to provide boundary conditions at the boundary of the fundamental domain to obtain a well-defined quantum mechanical problem. At weak coupling, the potential energy at the boundary of the fundamental domain is higher than the energy E of the wave function: the wave function is localized around the perturbative vacuum $c = d = 0$ and the boundary conditions are not felt.

Increasing the coupling results in the spreading of the wave function over the configuration space. We are interested in the regime where E is of the order of the sphaleron

energy: we will have a substantial flow of the wave function over the instanton barrier, but at the rest of the boundary the potential is still much higher than E . This means that at most parts of the boundary, the wave function will have decayed exponentially before reaching it. As a consequence, the boundary conditions imposed there will not have a large effect on the spectrum. By the same token, the precise location of the boundary in these regions is not important either. This gives us the freedom to choose tractable boundary conditions. At the sphalerons, however, the boundary conditions are fixed. Since the gauge transformation connecting the two sphalerons has winding number one, we have to set

$$(A(\text{Sph}; 0)) = e^{i\theta} (A(0; \text{Sph})); \quad (46)$$

thus introducing the angle.

We define radial coordinates r_c and r_d by

$$r_c = [c_1^a c_1^a]^{\frac{1}{2}}; \quad r_d = [d_1^a d_1^a]^{\frac{1}{2}}; \quad (47)$$

The sphaleron has radial coordinates $(\sqrt{3}; 0)$ and angular coordinates $\hat{c}_1^a = \frac{a}{i}$ (with $\hat{c}_1^a = \hat{c}_1^a = r_c$). It will be connected with the anti-sphaleron at $(0; \sqrt{3})$. We will restrict the $(r_c; r_d)$ plane by $r_c < \sqrt{3}$; $r_d < \sqrt{3}$ and impose boundary conditions at the edges. When we come to the variational calculation, we will use basis functions of the form $(r_c; r_d) Y(\hat{c}; \hat{d})$. As argued above, for values of the coupling constant at which our approximation will be valid, only the effect of the boundary conditions at the sphaleron will be felt. By imposing boundary conditions in the $(r_c; r_d)$ plane we pair up two submanifolds, of which only the sphaleron/anti-sphaleron need belong to the boundary of the fundamental domain.

Consider the following decomposition of the full wave function

$$= \frac{1}{r_c^4 r_d^4} \sum_{n=1}^{\infty} \psi^{(n)}(c; d) \phi^{(n)}(q); \quad (48)$$

where q denotes all the modes orthogonal to the c and d modes. This is just eq. (40) with an extra factor $r_c^4 r_d^4$ extracted for technical reasons (i.e. $\psi^{(n)} \propto r_c^{-4} r_d^{-4}$). Under the adiabatic approximation, we obtain a hamiltonian for $\psi = \psi^{(1)}$ given by

$$H = \frac{f}{2} \left(\frac{\partial^2}{\partial r_c^2} + \frac{\partial^2}{\partial r_d^2} \right) + 12 \left(\frac{1}{r_c^2} + \frac{1}{r_d^2} \right) + \frac{1}{r_c^2} \Delta_c + \frac{1}{r_d^2} \Delta_d + V(c; d); \quad (49)$$

with Δ_c the laplacian in the angular coordinates. The extra term $V^{(1)}(c; d)$ that one might expect is contained within $V(c; d)$.

The boundary condition on ψ follows directly from eq. (46), but care must be taken when imposing the condition on the normal derivative of ψ . Matching along the sphaleron path across the boundary of the fundamental domain, we need to compensate for the curvature with the appropriate jacobian factor. We will make this more precise.

Let us focus on the tunnelling path $c_1^a = u \frac{a}{i}$. Note that this path is equivalent to all paths $c_1^a = u S(\sim)_i^a$, with S an orthogonal matrix, due to the residual gauge symmetry. We will first remove this gauge symmetry to obtain a genuine one-dimensional tunnelling parameter. Introduce the following decomposition for c :

$$c = S(\rho) H(h_i); \quad S \in SO(3); \quad H^T = H; \quad (50)$$

If we write

$$H = \sum_{i=0}^5 h_i H_i; \quad (51)$$

with $\text{tr}(H_i H_j) = \delta_{ij}$ and with $H_0 = 1$, then h_0 will play the role of the gauge invariant tunnelling parameter. The sphaleron is located at $h_0 = \sqrt{3}$, $h_i = 0$; ($i = 1, \dots, 5$).

The isolation of the 18 (c;d) modes is appropriate close to the perturbative vacuum, because, as we have seen, they are the slow modes of the theory. Close to the sphaleron however, the only slow mode is the tunnelling mode $w = h_0 = \sqrt{3}$. To derive the correct boundary conditions, we should reduce the dynamics around the sphaleron to a one-dimensional tunnelling problem, by integrating out all other modes. To this end, we consider the following decomposition of :

$$\psi = \sum_n \psi_n^{(n)}(w) \phi_n^{(n)}(q); \quad (52)$$

where q not only denotes the non-(c;d) modes, but also the d modes and the h_i modes with $i = 1, \dots, 5$. Note that ψ does not depend on the gauge degrees of freedom θ_p . When imposing the boundary conditions, we want to relate the wave function at the sphaleron to the one at the anti-sphaleron. Consider the transverse modes q within the (c;d) space at the sphaleron. The gauge transformation that maps the sphaleron to the anti-sphaleron will not map these modes on modes within the (c;d) space at the anti-sphaleron: transverse modes inside and outside the (c;d) space get mixed under the gauge transformation. The transverse wave function at the sphaleron restricted to the (c;d) modes does therefore not map naturally to this transverse wave function at the anti-sphaleron. The full transverse wave functions do however map to each other. Another manifestation of this symmetry is the fact that the effective potential is symmetric around the sphaleron only when all transverse modes are integrated out.

Before going to the effective hamiltonian for $\psi^{(1)}(w)$ we must remove the residual gauge freedom. The gauge invariant wave function ψ is independent of the coordinates θ_p . We will show that only after a suitable rescaling of the wave function, the laplacian takes its cartesian form with respect to the tunnelling parameter w . The boundary conditions at the sphaleron must be imposed on this rescaled wave function.

Consider the laplacian for the c modes. If we write $u = (h_0, \dots, h_5; \theta_1, \theta_2, \theta_3)$ the laplacian takes the form

$$= \frac{1}{J} \partial_\mu (J g^{\mu\nu} \partial_\nu) : \quad (53)$$

Here $J = \det^{1/2}(g)$ and g is the metric which can be obtained from $d^2 = \text{tr}(\dot{u}\dot{u}) = g_{\mu\nu} \dot{u}^\mu \dot{u}^\nu$. For θ independent of w , one can show that at the sphaleron path eq. (53) reduces to

$$= \frac{1}{h_0^3} \partial_i h_0^3 \partial_i : \quad (54)$$

To obtain an ordinary one-dimensional tunnelling problem, we must rescale the wave function by $w^{3/2} / h_0^{3/2}$:

$$\psi(w) = w^{-3/2} \tilde{\psi}(w) : \quad (55)$$

The tunnelling problem then looks as

$$\frac{1}{2} \frac{\partial^2}{\partial w^2} + V(w) \psi(w) = E \psi(w): \quad (56)$$

We can derive a similar equation for a function ψ^0 of the parameter w^0 corresponding to tunnelling through the anti-sphaleron. When matching these tunnelling paths through the relation $w^0 = 2 - w$, boundary conditions must be imposed on ψ and on its normal derivative at the sphaleron $w = 1$. Combining the factors $w^{3/2}$ and r^{-4} leads to the following boundary conditions on ψ :

$$(\text{Sph}; 0) = e^i (0; \text{Sph}); \quad (57)$$

$$\frac{\partial (r_c^{5/2})}{\partial r_c} (\text{Sph}; 0) = e^i \frac{\partial (r_d^{5/2})}{\partial r_d} (0; \text{Sph}): \quad (58)$$

3 The one-loop effective lagrangian

3.1 Introduction

In this section we will calculate the influence of the high-energy modes on the dynamics of the low-energy modes [18]. This is achieved by integrating out the high-energy modes in the path integral, which gives us the one-loop effective lagrangian for the low-energy modes. Denoting the low-energy modes by $B(c; d)$, we will expand the one-loop effective lagrangian first up to the same order as the classical potential, i.e. up to fourth order in B and to second order in B^- . This allows us to do the renormalization of the lagrangian properly.

Since we expect the physics to be sensitive to the details of the potential along the tunnelling path, we use an expansion of the effective potential around the sphaleron to construct a fit of the effective potential up to sixth order in the tunnelling parameter u . This allows us to write down the effective lagrangian including some fifth and sixth order terms in B so as to reproduce the behaviour along the tunneling path.

It is our purpose to use the effective hamiltonian in a variational method to calculate the spectrum. Although it is possible to calculate the effective potential exactly along the tunnelling path, a polynomial approximation in B is much more useful, since this makes the analytic evaluation of the matrix elements feasible.

The one-loop effective lagrangian will be given in terms of a path integral over the high-energy modes and over ghost fields. Using Feynman diagrams to expand these path integrals is the standard method to proceed, but due to the fact that the theory is defined on S^3 , the summation over the space components of a loop momentum looks rather different from the more familiar summation over the time component. To isolate the intricacies of the three-sphere, we will first assume B to be time independent. This allows us to perform the integrations over time components of loop momenta. Within this so-called adiabatic approximation the calculation of the effective potential as an expansion in B is then a purely algebraic problem.

After this we return to the use of Feynman diagrams to evaluate the one-loop contribution to the kinetic term. We will neglect higher order time derivatives of B and also

terms of the form $B^n B^2$. We choose a renormalization scheme that makes the renormalized kinetic part assume the form of the classical kinetic term, replacing the bare by the renormalized coupling constant. The result of this section is then a finite, renormalized effective action.

3.2 Gauge fixing

We will impose the background gauge condition on the high-energy modes. Consider a general gauge field $A = (A_0; A_i)$ on S^3 , where A_0 is the time component of the gauge field and A_i are the space components with respect to the framing e^i . We will project out the background field $B(c; d)$. Let P_S be the projector on the constant scalar modes, and let $P_V = P_C + P_d$ be the projector on the $(c; d)$ -space. Explicitly we have:

$$P_S = P_0^L = \frac{1}{2^2} \int_{S^3} ; \quad (59)$$

$$(P_C A)_i = P_0^L A_i = \frac{1}{2^2} \int_{S^3} A_i; \quad (60)$$

$$(P_d A)_i = P_0^K A_i = \frac{1}{2^2} \int_{S^3} A_k V_k^1 V_i^1; \quad (61)$$

We define the background field B and the quantum field Q by respectively

$$B = (P A) = (P_S A_0; (P_V A)_i); \quad Q = A - B; \quad (62)$$

We define the gauge fixing function $\chi = (1 - P_S) D(P A) A + P_S A_0$. We use χ to impose the background gauge condition:

$$\begin{aligned} \chi &= 0, \quad \int_{S^3} B_0 = 0 \\ \chi &= 0, \quad \int_{S^3} D(B) Q = 0 \end{aligned} \quad (63)$$

Introducing the Faddeev-Popov determinant

$$[A] = \int_{S^3} Dg[A]; \quad (64)$$

and performing the standard manipulations with the partition function leads to

$$Z = \int_{S^3} DB_k DQ [A] \exp \left[-\frac{1}{2g_0^2} \int_{S^3} \text{tr} \frac{1}{2} F^2(B + Q) + \frac{1}{2} \int_{S^3} (D(B)Q)^2 \right]; \quad (65)$$

The primed integration means that we have excluded the $l=0$ modes from the integration over the scalar field Q_0 and the $l=0; k=1$ and $l=1; k=0$ modes (the $(c; d)$ modes) from the integration over the vector field Q_k .

We now focus on the Faddeev-Popov determinant (64). Under an infinitesimal gauge transformation the change in A is given by $D(A)$ and the change in the gauge fixing function by

$$\begin{aligned} \delta \chi &= - \\ &= (1 - P_S) f D(P A) D(A) + [P D(A)] A + P_S D_0(A) \end{aligned}$$

$$\begin{aligned}
&= (1 - P_S) fD(B) D(A) [B; (PD(A))] \\
&\quad Q; (PD(A))] \int + P_S D_0(A) \\
&= (1 - P_S) fD(B) (1 - P) D(A) + Q (PD(A)) \\
&\quad Q; (PD(A))] \int + P_S D_0(A) \\
&= (1 - P_S) fD(B) (1 - P) D(A) [Q; (PD(A))] \int \\
&\quad + P_S D_0(A) : \tag{66}
\end{aligned}$$

The Faddeev-Popov determinant is given by $[A] = \det(\dots)$. Introducing ghost fields and \bar{c} , this determinant can be written as a fermionic path integral. We will evaluate this path integral in the quadratic approximation, that is, we throw away terms of order three and higher in the quantum fields and Q . After this the integration over the $l=0$ modes of \bar{c} can be performed to give an irrelevant constant and we obtain

$$[A] / \int D^0 D^0 \exp \int \text{tr} D(B) (1 - P) D(B) : \tag{67}$$

Substituting this in the partition function with $\beta = 1/g_0^2$, expanding the classical euclidean action up to second order in Q , and choosing the Feynman gauge $\beta = 1$ we obtain

$$\begin{aligned}
Z &= \int D B_k D Q D^0 D^0 \exp \frac{1}{g_0^2} \int \text{tr} f D(B) (1 - P) D(B) g \\
&\quad + \frac{1}{2} F^2(B) - 2(D \cdot F)(B) Q + Q W(B) Q ; \tag{68}
\end{aligned}$$

with

$$\begin{aligned}
W_{00} &= D^2(B) \\
W_{0i} &= W_{i0} = 2 \text{ad}(B_i) \\
W_{ij} &= 2 \text{ad}(F_{ij}(B)) - (D^2(B))_{ij} + 2 \delta_{ij} \tag{69}
\end{aligned}$$

Remember that the covariant derivative $D_i(B)$ acting on vectors (or tensors) gives extra connection terms (due to S^3 being a curved manifold), e.g.

$$(D_i(B) C)_j = \partial_i C_j + [B_i; C_j] - \epsilon_{ijk} C_k \tag{70}$$

$$= (-2iL_i + iB_i^a T^a - iS_i)_{jk} C_k \tag{71}$$

The action contains a term $\int Q$ with $J = (D \cdot F)(B)$. Since B need not satisfy the equations of motion, this term does not vanish. Upon expanding the path integral in Feynman diagrams, this term will give rise to extra diagrams, where J acts as a source. In appendix B we will show that the presence of J will only contribute to terms in the effective lagrangian that we will consider to give only small corrections: they are at least of order $c^2 d^4$ or $c^4 d^2$.

Dropping for the time being the term linear in Q , we are left with a gaussian integration over the fields and Q from which we extract the effective action

$$\begin{aligned}
S_E^{\text{eff}}[B] &= \int_0^T \int d^3x (K + V) \\
&= S_E^{\text{cl}}[B] - \ln \det(D(B) (1 - P) D(B)) + \frac{1}{2} \ln \det(W) : \tag{72}
\end{aligned}$$

Although we will not use the primed notation to denote it, the determinant does exclude the same modes that were not integrated over in the path integral.

3.3 The effective potential

For computing the effective potential, B is considered to be independent of time. The assumption $B_- = 0$ directly implies $W_{0i} = 0$. This results in a factorization of the integral over Q , and we obtain the one-loop contribution to the effective action

$$S_E^{(1)}[B; B_- = 0] = -\ln \det (D(B)(1 - P)D(B)) + \frac{1}{2} \ln \det (D(B)D(B)) + \frac{1}{2} \ln \det (W_{ij}) : \quad (73)$$

We have to calculate these functional determinants for a general background $B(c; d)$.

3.3.1 The operators

We start by expressing the various operators of eq. (73) in terms of c and d . For the scalar operator $W_{00} = D^2(B)$ we find

$$D(B)D(B) = \partial_0^2 D_i(B)D_i(B) : \quad (74)$$

As it acts on scalar functions, we have $D_i(B) = 2iL_i + iB_i^a T^a$ and we obtain

$$\begin{aligned} D_i(B)D_i(B) &= 4L^2 - 4B_i^a L_i T^a + B_i^a B_i^b T^a T^b \\ &= 4L^2 - 4c_1^a L_{1i} T^a - 4d_1^a L_{2i} T^a \\ &\quad + c_1^a c_1^b + d_1^a d_1^b + c_1^a d_m^b V_i^m + d_m^a V_i^m c_1^b T^a T^b : \end{aligned} \quad (75)$$

The other scalar operator (the ghost operator) can also be written as

$$D(B)(1 - P)D(B) = \partial_0^2 D_i(B)(1 - P_V)D_i(B) ; \quad (76)$$

where use was made of the fact that the operator does not act on constant functions. Carefully analysing the extra term allows us to write

$$\begin{aligned} D_i(B)P_V D_i(B) &= P_1^L D_i(B)(P_V)_{ij} D_j(B)P_1^L \\ &= \frac{1}{3} c_1^a c_1^b - c_1^a c_j^b L_{1j} L_{1i} + d_1^a d_1^b - d_1^a d_j^b L_{2j} L_{2i} T^a T^b P_1^L : \end{aligned} \quad (77)$$

The vector operator W_{ij} is more complicated due to the extra connection terms. We write

$$W_{ij} = \partial_0^2 \delta_{ij} + \tilde{W}_{ij} ; \quad (78)$$

Using the spin operator S we can suppress the spin-indices and write

$$\begin{aligned} \tilde{W}(B) &= 2L^2 + 2K^2 - 4c_k^a L_{1k} T^a - 4d_k^a L_{2k} T^a + (6c_k^a + 2d_m^a V_k^m) S_k T^a \\ &\quad + \frac{1}{2} \epsilon_{ijk} \epsilon_{abc} c_i^a c_j^b - 2 \epsilon_{ijk} \epsilon_{abc} c_i^a d_m^b V_j^m + \frac{1}{2} \epsilon_{lmn} \epsilon_{abc} d_l^a d_m^b V_k^n S_k T^c \\ &\quad + c_k^a c_k^b + d_k^a d_k^b + c_k^a d_m^b V_k^m + d_m^a V_k^m c_k^b T^a T^b : \end{aligned} \quad (79)$$

3.3.2 Reduction to spatial parts

As we have seen, the operators we are interested in are of the form

$$A(B) = \partial_0^2 - \partial_n^2 + \tilde{A}(B); \quad (80)$$

where we introduced a laplacian term for an n -dimensional torus of size L that we attached to our space S^3 [23]. This allows us to neatly perform the dimensional regularization. The scale L should of course be chosen proportional to the radius R of the three-sphere. A precise choice of L would fix our regularization procedure completely, and different choices will be related through finite renormalizations fixing the relations between the associated parameters.

Suppose that the spectrum of \tilde{A} is $f_i g$. The spectrum of ∂_n^2 is $f k_n^2 g$ with $k_n = 2\pi n/L$. If we also take the time periodic with period T , the spectrum of ∂_0^2 is $f k_0^2 g$ with $k_0 = 2\pi n/T$. Since $[\partial_0, \tilde{A}(B)] = [\partial_n, \tilde{A}(B)] = 0$, the spectrum $f_i g$ of $A(B)$ follows trivially.

Consider the exponential integral

$$E_1(x) = \int_0^\infty \frac{ds}{s} e^{-sx} = -\ln(x) - \sum_{n=1}^\infty \frac{(-1)^n x^n}{n n!}; \quad (81)$$

This implies

$$\int_0^\infty \frac{ds}{s} e^{-s} = -\ln(1) - \ln(1) + O(1); \quad (82)$$

Taking the limit $\epsilon \rightarrow 0$ in this integral, we can write, up to an irrelevant constant,

$$\begin{aligned} \ln \det(A) &= \sum_i \ln(f_i) \\ &= \sum_{k_0, k_n} \int_0^\infty \frac{ds}{s} e^{-s(k_0^2 + k_n^2 + f_i)} \\ &= \frac{T}{2} \sum_{k_0} \frac{L^n}{2} \sum_{k_n} \int_0^\infty ds s^{-\frac{3}{2} - \frac{n}{2}} \text{tr} e^{-s\tilde{A}} \end{aligned} \quad (83)$$

where we replaced the summations over k_0 and k_n by integrals. The operator \tilde{A} can be expressed in terms of the angular momentum operators defined above, the functions V_i^j and the constants c_i^a and d_i^a . To take the trace, we need a basis of functions (see section 2). For the scalar operators (the ghost operator and W_{00}), we can use $|j m_L m_R i\rangle$ or equivalently $|j m_R; j m_j i\rangle$, where m_L, m_R and m_j correspond to the z -components of \tilde{L}_1, \tilde{L}_2 and $\tilde{J} = \tilde{L}_1 + \tilde{L}_2$ respectively. For the vector operator W_{ij} , we can use $|j m_R; k m_k i\rangle$ or $|j m_R; k; j m_j i\rangle$. Note that the c and d modes correspond to the vector modes with $(l; k) = (0; 1)$ and $(l; k) = (1; 0)$ respectively. For the scalar operators, the trace must not be taken over the $l=0$ functions, whereas for the vector operator the trace must not include the c and d modes. For the case of the ghost operator, the operator $(1 - P)$ (see eq. (76)) causes some intermediate vector modes to be projected to zero.

3.3.3 Exact determinants

Using the appropriate basis, we can calculate the determinants exactly for the vacuum $u = 0$ ($B = 0$), and for the sphaleron configuration $u = 1$ ($\alpha_1^a = \frac{a}{i}$ and $d = 0$). After integrating over s , the final summation over l is expressed in terms of the function $(s; a)$, which is defined by

$$(s; a) = \sum_{k=2}^{\infty} \frac{1}{(k^2 + a)^s}; \quad \text{Re}(s) > \frac{1}{2}; \quad (84)$$

After analytic continuation we have

$$(s; a) = \sum_{m=0}^{\infty} \frac{(s)_m}{m!} (-a)^m (-\zeta_R(2s + 2m - 1)); \quad s \notin \frac{1}{2}; \frac{1}{2}; \dots; \quad (85)$$

where ζ_R denotes the Riemann ζ -function and $(s)_m$ is Pochhammer's symbol. If s approaches one of the poles, this expansion can be used to split off the divergent term: the remainder of the series is denoted with $\zeta_F(s; a)$. As an example we treat W ($B = 0$) = $\mathcal{Q}_0^2 + 2L^2 + 2K^2$. From eq. (83) we obtain

$$\begin{aligned} \ln \det(W_{ij}) &= \sum_{l=1}^{\infty} \sum_{k=1}^{\infty} \left(\frac{1}{2} - \frac{n}{2} \right) \text{tr} (2L^2 + 2K^2)^{\frac{1}{2} + \frac{n}{2}} \\ &= \sum_{l=1}^{\infty} \sum_{k=1}^{\infty} \left(\frac{1}{2} - \frac{n}{2} \right) 3^{\sum_{l,k} \frac{(2l+1)(2k+1)}{(2l(l+1) + 2k(k+1))^{\frac{1}{2} + \frac{n}{2}}}} : \\ &= \sum_{l=1}^{\infty} \sum_{k=1}^{\infty} \left(\frac{1}{2} - \frac{n}{2} \right) 3^{\left(\frac{3}{2} - \frac{n}{2}; 1 \right) + 3 \left(\frac{1}{2} - \frac{n}{2}; 1 \right)} \\ &\quad + 6 \left(\zeta_R \left(3 - \frac{n}{2} \right) - 9 \right) - 6 \left(\zeta_R \left(1 - \frac{n}{2} \right) - 3 \right) : \end{aligned} \quad (86)$$

The summation over $(l; k)$ is as follows:

$$\sum_{l,k} = \sum_{m=\frac{1}{2}, 1, \dots}^{\infty} \left(\sum_{l+m=k} 1 + \sum_{l+m+1=k} 1 + \sum_{l+m=k+1} 1 \right) : \quad (87)$$

Using similar techniques for the other cases, we find for the effective potentials

$$V^{(1)}(B = 0) = \frac{18 + 3 \zeta_R(-3)}{3^{\frac{p}{2}}} - \frac{3 \zeta_R(-1)}{12^{\frac{p}{3}}} + \frac{9^{\frac{p}{6}}}{2^{\frac{5p}{2}}} \frac{1}{10} + \frac{11}{4} \frac{1}{8} + \frac{11}{4} \log(2) \quad (88)$$

$$\begin{aligned} V^{(1)}(\text{Sph}) &= \frac{1}{3^{\frac{p}{2}}} - \frac{1}{12^{\frac{p}{3}}} + \frac{9^{\frac{p}{6}}}{2^{\frac{5p}{2}}} \frac{1}{10} + \frac{11}{4} \frac{1}{8} + \frac{11}{4} \log(2) \\ &\quad + \frac{11}{4} \log \frac{\zeta_F(\frac{3}{2}; 3)}{\zeta_F(\frac{3}{2}; 2)} + \zeta_F\left(\frac{3}{2}; 3\right) + \zeta_F\left(\frac{3}{2}; 2\right) + \zeta_F\left(\frac{3}{2}; 1\right) \\ &\quad + 3 \zeta_F\left(\frac{1}{2}; 3\right) + \zeta_F\left(\frac{1}{2}; 2\right) - 5 \zeta_F\left(\frac{1}{2}; 1\right) \end{aligned} \quad (89)$$

The pole term $\frac{11}{4} \frac{1}{n}$ has to be absorbed through a renormalization of the coupling constant. Adding the classical potential at the sphaleron we get

$$V_e(\text{Sph}) = \frac{2}{g_0^2} \frac{3}{2} + \frac{11}{4} \frac{1}{n} + \text{finite renormalization} : \quad (90)$$

So the infinite part of the renormalization is

$$\frac{1}{g_R^2} = \frac{1}{g_0^2} + \frac{11}{12^{\frac{p}{2}}} \frac{1}{n} : \quad (91)$$

This is the standard result for SU(2) gauge theory in 1 + 3 dimensions as of course it should be: the renormalization is an ultra-violet effect and does not depend on the global properties of the space on which the theory is defined.

3.3.4 General background field

For a configuration along the tunneling path, $c_i^a = u \frac{a}{i}$, $d = 0$, we make an expansion of the eigenvalues of the operators in u . The operators are:

$$D_i(u)D_i(u) = 4L^2 + 4uL \cdot T + 2u^2; \quad (92)$$

$$D_i(u)(1 - P_V)D_i(u) = 4L^2 + 4uL \cdot T + 2u^2 + \frac{1}{3}u^2 \frac{2}{3}(L \cdot T)^2 - L \cdot T \cdot P_1^L; \quad (93)$$

$$\tilde{W}(u) = 2L^2 + 2K^2 + 4uL \cdot T + (6u - 2u^2)S \cdot T + 2u^2; \quad (94)$$

From eq. (92) it directly follows that the eigenfunctions of the scalar operator $\tilde{A} = D_i(B)D_i(B)$ are the $|j m_R; j m_j\rangle$ with the eigenvalues $4l(l+1) + 2u(j(j+1) - l(l+1) - 2) + 2u^2$. This allows us to write in eq. (83)

$$\text{tr } e^{-s\tilde{A}} = \sum_{l=\frac{1}{2}, 1, \dots}^{\infty} (2l+1) e^{-s4l(l+1)} \sum_{j=l-1}^{l+1} (2j+1) e^{-s(2u(j(j+1) - l(l+1) - 2) + 2u^2)}; \quad (95)$$

and to expand the second exponential in u . After performing the summation over j and the integration over s , the l -summations can again be expressed in terms of ζ -functions. Most of the algebra was done using FORM [24]. The other scalar operator can be treated similarly. The eigenvalues can be written down from eq. (93) as well: they differ from the ones above only for $l=1$.

For the vector operator the situation is more complicated since the eigenvalues are not readily available. We write

$$\tilde{W}(u) = 2L^2 + 2K^2 + \hat{W}(u); \quad (96)$$

where the precise form of $\hat{W}(u)$ can be read off from eq. (94). Since $\hat{W}(0) = 0$ we can treat $\hat{W}(u)$ as a perturbation on the operator $2L^2 + 2K^2$. As \tilde{W} commutes with the $fL^2; L_{2z}; J^2; J_z$, the basis to use is $|j(l)k; j\rangle$. The dimension for the subspace in which we have to find the eigenvalues of \tilde{W} is given by the number of possible k values. Since this dimension is maximally three, it is of course possible to obtain the eigenvalues of $\tilde{W}(u)$ exactly, but as explained earlier, it is more convenient to expand in u . The unperturbed eigenvalues within each sector are $2l(l+1) + 2k(k+1)$, so we need non-degenerate perturbation theory to obtain the expansion in u for the eigenvalues $\tilde{\omega}(j; k; l)$. A method that implements this particularly nice is due to Bloch [25]

Using MATHEMATICA [26] we computed the expansions for the eigenvalues. For this we needed the matrix elements of the operators $L \cdot T$ and $S \cdot T$. To calculate these matrix elements, we need the 6- j symbols [27]. For three angular momenta $t; s$ and l we have (cf. section 2)

$$j; (sl)k; ji = \sum_q (-1)^{t+s+l+j} [(2q+1)(2k+1)]^{\frac{1}{2}} \begin{matrix} 8 \\ < \\ t & s & q \\ 1 & j & k \end{matrix} \begin{matrix} 9 \\ = \\ j(ts)q; l; ji \end{matrix} \quad (97)$$

This gives

$$\begin{aligned} \text{ht}(sl k^0; jjS \quad T \quad j; sl k; ji) &= \frac{1}{2} (s(s+1) + t(t+1)) \quad k^0_k \\ &+ \frac{1}{2} \sum_q q(q+1)(2q+1)[(2k+1)(2k^0+1)]^{\frac{1}{2}} : \begin{matrix} 8 & 9 & 8 & 9 \\ t & s & q & = < t & s & q & = \\ 1 & j & k^0 & ; & 1 & j & k & ; \end{matrix} : \quad (98) \end{aligned}$$

The matrix elements for \mathbb{L} and \mathbb{T} follow from this and the identity $\mathbb{J}^2 = \mathbb{K}^2 + \mathbb{T}^2 + 2\mathbb{L} \cdot \mathbb{T} + 2\mathbb{S} \cdot \mathbb{T}$. As in the case of the scalar operators, we expand the exponential in u and perform the s -integration. The summations over l can be expressed in γ -functions. During the various stages of these calculations care has to be taken for low values of l ; k and j : for certain values the Bloch result for the general eigenvalue $\sim (j; k; l)$ will not be valid, since the subspace in which to perform the diagonalization may have less dimensions than the bulk value $3 - j_l - j_j$: some of the k values would be negative. Moreover, in the $l = 1, j = 1$ sector, which is a priori three dimensional, the $k = 0$ modes have to be thrown out explicitly, since they are the d modes. Exclusion of the c modes is simply achieved by starting the summation over l with $l = \frac{1}{2}$. The result for the effective potential up to fourth order in u is

$$\begin{aligned}
V^{(1)}(u) = & 18 + 3 \, {}_R(3) - 3 \, {}_R(1) \\
& + V_{cl}(u) \left[\frac{1259}{1152} + \frac{11}{6} {}_R(2) - \frac{11}{12} {}_R(1) - \frac{11}{128} P_2 + \frac{11}{6} \log(2) + \frac{11}{6} \log \frac{u}{2} \right] \\
& + \frac{23}{6} \left(\frac{3}{2}; 1 \right) - \frac{1}{6} \left(\frac{5}{2}; 1 \right) + \frac{53}{3} \left(\frac{7}{2}; 1 \right) + 14 \left(\frac{9}{2}; 1 \right) \\
& + \frac{16}{3} \, {}_R(3) - \frac{19}{6} \, {}_R(5) - \frac{1}{3} \, {}_R(7) \\
& + u^2 \left[\frac{179}{192} + \frac{33}{64} P_2 + 13 \left(\frac{3}{2}; 1 \right) - 9 \left(\frac{5}{2}; 1 \right) - 106 \left(\frac{7}{2}; 1 \right) \right. \\
& \quad \left. - 84 \left(\frac{9}{2}; 1 \right) + 2 \, {}_R(1) - 23 \, {}_R(3) + 19 \, {}_R(5) + 2 \, {}_R(7) \right] \\
& + u^4 \left[\frac{863}{768} + \frac{1475}{2048} P_2 - \frac{53}{4} \left(\frac{3}{2}; 1 \right) + \frac{17}{4} \left(\frac{5}{2}; 1 \right) + \frac{261}{2} \left(\frac{7}{2}; 1 \right) \right. \\
& \quad \left. + 47 \left(\frac{9}{2}; 1 \right) - 66 \left(\frac{11}{2}; 1 \right) + \frac{63}{4} \, {}_R(3) - 79 \, {}_R(5) \right. \\
& \quad \left. + \frac{227}{4} \, {}_R(7) + 5 \, {}_R(9) \right] :
\end{aligned} \tag{99}$$

Here we eliminated the u^3 term in favour of the classical potential V_{cl} defined by

$$V_{cl} = \frac{2}{g_0^2} V_{cl} i \quad (100)$$

SO

$$V_{cl}(u) = \frac{3}{2}u^2(2-u)^2: \quad (101)$$

One checks that the pole term is absorbed by the coupling constant renormalization of eq. (91).

Results up to tenth order in u were calculated. As can be seen from fig. 2, the expansions do not converge to the exact result at $u = 1$. This should come as no big surprise, since we have no reason to expect the radius of convergence of the expansion to be as large as one. Judging from the picture, one would estimate a radius of convergence of roughly 0.6.

To find the effective potential for larger u , we make a similar expansion of the effective potential around the sphaleron: $u = 1 + a$. The expansions of the determinants of the scalar operators can be obtained exactly as described above. The final summations can be expressed in terms of $(s; b)$ with $b = 3; 2; 1$. For the vector operator, we could in principle again use the Bloch perturbation method to obtain the eigenvalues $\tilde{\omega}(j; k; l)(a)$, although the levels are now degenerate at $a = 0$. There is however an easier way. Suppose we have $\tilde{A} = F + \hat{A}$ with $F = \tilde{A}(0)$ such that $[F, \hat{A}] = 0$. This allows us to substitute in eq. (83)

$$\text{tr } e^{-s\tilde{A}} = \text{tr } e^{-sF} e^{-s\hat{A}} = \sum_i e^{-sF_i} \sum_{n=0}^{\infty} \frac{(-s)^n}{n!} \text{tr}_i \hat{A}^n : \quad (102)$$

The sum over i is a sum over the eigenspaces of F , F_i is the corresponding eigenvalue and $\text{tr}_i()$ denotes a trace within the eigenspace. For the operator W

$$W(a) = 2L^2 + 2J^2 - 2 + a(4 + 4L \cdot T + 2S \cdot T) + a^2(2 - 2S \cdot T); \quad (103)$$

we indeed have that $F = W(0) = 2L^2 + 2J^2 - 2$ commutes with \hat{W} and we obtain

$$\begin{aligned} \ln \det(W) &= \frac{\text{Tr}}{2} = \frac{\text{Tr}}{2} = \sum_{l,j} \sum_{k=0}^{\infty} (2l+1)(2j+1) \\ &\int_0^{\infty} ds s^{\frac{3}{2}} e^{-s(2l(2l+1)+2j(2j+1)-2)} \sum_{n=0}^{\infty} \frac{(-s)^n}{n!} \text{tr}_{lj} \hat{W}^n : \end{aligned} \quad (104)$$

Note that the sum over different k values is now absorbed in the trace in the $(l; j)$ space. When taking this trace one has to deal with the same subtleties connected with low values of l and j as described before. The resulting effective potential is an expansion in a . Its behaviour is similar to that of the previous expansion: we have a radius of convergence of roughly 0.4 around the sphaleron $u = 1$. Using the fourth order expansion in u and the first order expansion in a (i.e. the value and the slope of the potential at the sphaleron), we can construct a polynomial in u of degree six that is a good approximation to the effective potential.

Regarding the issue of the radius of convergence, one might think that also integrating out the $(c; d)$ modes that are orthogonal to the u mode might result in better convergence. Also one expects the $u \rightarrow -u$ symmetry to be restored in this case. With the techniques described above, performing this calculation is straightforward, provided one remembers to properly adjust the gauge fixing procedure. The new expansions in u and a have roughly the same convergence behaviour as before, so there is no improvement on this point. The symmetry is however manifestly restored: the expansion in a contains only even powers of a .

For the case of the vacuum and the sphaleron configuration, we could calculate the spectra of the operators exactly. For a configuration along the tunnelling path, the operators have less symmetries, and the evaluation of the spectra becomes harder. For $B = B(c; d = 0)$ and especially $B = B(c; d)$ we have even fewer operators that commute with the operators whose determinants we want to calculate. Nevertheless, we developed methods [18, 28] to calculate the functional determinants up to fourth order in c and d . These methods are based on eq. (102) and a generalization thereof. We postpone writing down the result of this calculation, which is the effective potential, until we have performed the renormalization.

3.4 The effective kinetic term

To obtain the one-loop contribution to the operator B^2 , we perform the usual expansion of the path integral in Feynman diagrams. The subtleties related to the summation over the space-momenta were dealt with in the previous section. The diagrams needed are simple loop diagrams with one and two insertions of the operator \hat{A} defined above. The particle in the loop is respectively a ghost, a scalar Q_0 or a vector particle. The B^2 term comes from the diagrams with two insertions.

As an example we will treat the diagram d_2 with two ghost propagators and two insertions of the operator \hat{A} . The fermionic path integral is given by

$$\begin{aligned} Z &= \int D^0 D^0 \exp \frac{1}{g_0^2} \text{tr} \int_0^1 dt \int_0^1 dt^0 \text{tr} \left(\mathcal{D}^0(B)(1-P)\mathcal{D}^0(B)g \right) \\ &= \int D^0 D^0 \exp \frac{1}{g_0^2} \text{tr} \int_0^1 dt \int_0^1 dt^0 \left(\mathcal{D}_0^2 - \mathcal{D}_0^2 + 4\mathcal{L}^2 + \hat{A} \right) : \end{aligned} \quad (105)$$

The propagator in momentum space is given by

$$\frac{1}{k_0^2 + k_n^2 + 4l(l+1)} : \quad (106)$$

We will suppress the manipulations with the integrations over k_n and x_n . The dimensional regularization can be obtained by adding k_n^2 to the denominators of all propagators and performing the integration

$$L = \int \frac{d^4 k_n}{(2\pi)^4} : \quad (107)$$

Suppressing m_L , m_R and m_t , we find for the diagram with two insertions

$$\begin{aligned} d_2 &= \frac{1}{2} \int_0^1 dt \int_0^1 dt^0 \frac{dk_0}{2} \frac{dk_0^0}{2} \int_0^1 dx \int_0^1 dx^0 \frac{1}{k_0^2 + 4l(l+1)} \text{tr} \left(\hat{A}(t^0) \mathcal{D}^0(t-t^0) \right) \\ &= \frac{1}{k_0^2 + 4l(l+1)} \text{tr} \int_0^1 dt \int_0^1 dt^0 \hat{A}(t) \mathcal{D}^0(t-t^0) : \end{aligned} \quad (108)$$

Noting that $\mathcal{L}^2 \hat{A}(t) = 0$ and substituting $k_0 = p$, $k_0^0 = p + q$ we write

$$\begin{aligned} d_2 &= \frac{1}{2} \int_0^1 dt \int_0^1 dt^0 \frac{dp}{2} \frac{dq}{2} \int_0^1 dx \int_0^1 dx^0 \text{tr} \left(\hat{A}(t) \hat{A}(t^0) \right) \\ &= \frac{1}{p^2 + 4l(l+1)} \frac{1}{(p+q)^2 + 4l(l+1)} : \end{aligned} \quad (109)$$

Using contour integration, one proves

$$\int_0^1 \frac{dp}{2} \frac{1}{p^2 + C} \frac{1}{(p+q)^2 + C} = \frac{1}{C} \frac{1}{(4C + q^2)} : \quad (110)$$

After performing the p integration and expanding in q^2 we obtain

$$\begin{aligned} d_2 &= \frac{1}{2} \int_0^1 dt \int_0^1 dt^0 \frac{dq}{2} \int_0^1 dx \int_0^1 dx^0 \text{tr} \left(\hat{A}(t) \hat{A}(t^0) \right) \\ &= \frac{1}{4(4l(l+1))^{\frac{3}{2}}} \sum_{n=0}^{\infty} \frac{(-1)^n}{4^n} \frac{(q^2)^n}{(4l(l+1))^n} : \end{aligned} \quad (111)$$

Next we substitute

$$q^2 \rightarrow \frac{\partial^2}{\partial t \partial t^0}; \quad (112)$$

and move these time derivatives to \hat{A} by partial integration. The q and the t^0 integration thus become trivial, and we obtain

$$\begin{aligned} d_2 &= \frac{1}{8} \int_0^Z dt \int_{-1}^1 dx \int_{-1}^1 dx' \frac{(-1)^n}{4^n} \frac{1}{(4l(l+1))^{n+\frac{3}{2}}} \text{tr}_1 \hat{A}^{(n)}(t) \hat{A}^{(n)}(t) \\ &\rightarrow \frac{1}{8} \int_0^Z dt \int_{-1}^1 dx \int_{-1}^1 dx' \frac{(-1)^n}{4^n} \frac{g_{n+\frac{3}{2}}''}{(4l(l+1))^{n+\frac{3}{2}+\frac{n}{2}}} \text{tr}_1 \hat{A}^{(n)}(t) \hat{A}^{(n)}(t) : \end{aligned} \quad (113)$$

The arrow indicates that we have performed the n -dimensional integrations that were suppressed in the notation. We introduced

$$g_n'' = \int_0^Z dx'' \int_0^Z dx''' \frac{d^2 k''}{(2\pi)^n} \frac{1}{(1+k''^2)^n} = \frac{1}{2^n} \frac{\Gamma(\frac{n}{2})}{\Gamma(n)} : \quad (114)$$

The $n=0$ contribution in eq. (113) can be related to the s^2 term in eq. (102), whereas the $n=1$ contribution gives us the B^2 term that we were looking for:

$$\int_0^Z dt \frac{1}{12} g_{\frac{5}{2}}'' = \left(\frac{1}{2} - \frac{n}{2}; 1\right) + \left(\frac{3}{2} - \frac{n}{2}; 1\right) \frac{c_4^a c_4^a}{4} : \quad (115)$$

The bosonic path integral is given by

$$\begin{aligned} Z &= \int_0^Z DQ \exp \frac{1}{g_0^2} \int_0^Z \text{tr} (2(D \cdot F)(B)Q + QW(B)Q) \\ &= \int_0^Z DQ_0 DQ_i \exp \frac{1}{g_0^2} \int_0^Z \text{tr} Q_0^2 \left(\mathcal{E}_0^2 + 4\mathcal{L}^2 Q_0 \right. \\ &\quad \left. + Q_i^2 \left(\mathcal{E}_0^2 + 2\mathcal{L}^2 + 2\mathcal{K}^2 \right)_{ij} Q_j + Q_0 \hat{A} Q_0 + Q_i \hat{W}_{ij} Q_j \right. \\ &\quad \left. + 4Q_0 \text{ad}(B_j)Q_j - 2J_0 Q_0 - 2J_i Q_i \right) : \end{aligned} \quad (116)$$

with $J = (D \cdot F)(B)$ (see appendix B). The diagrams where the particle in the loop is a Q_0 particle have the same structure as those with a ghost particle. Apart from extra terms coming from the projector $1 - P$ in the ghost case, the contribution is precisely $\frac{1}{2}$ times the fermionic contribution. The diagram with a vector particle gives rise to some extra technical problems, but it can also be dealt with. There is also a diagram with an explicit dependence on B : it is the diagram with two insertions of the operator $W_{0i} / \text{ad}(B_i)$, one Q_0 and one Q_i propagator.

Adding up the different contributions, we obtain the one-loop contribution to the kinetic term $c_4^a c_4^a + d_1^a d_1^a$ in the lagrangian:

$$\begin{aligned} K^{(1)}(c;d) &= c_4^a c_4^a + d_1^a d_1^a - \frac{1247}{1152} + \frac{5}{16} P - \frac{11}{12} \frac{11}{24} + \frac{11}{12} \log(2) \\ &\quad + \frac{11}{12} \log\left(\frac{1}{2}\right) + \frac{1}{6} \left(\frac{3}{2}; 1\right) + 11 \left(\frac{5}{2}; 1\right) + \frac{49}{6} \left(\frac{7}{2}; 1\right) \\ &\quad - \frac{4}{3} R(3) - \frac{5}{12} R(5) - \frac{8}{3} F\left(\frac{1}{2}; 1\right) : \end{aligned} \quad (117)$$

The divergency will be absorbed by the same coupling constant renormalization of eq. (91) that also made the potential part finite.

$c_0 =$	0.0566264741439181
$c_1 =$	0.2453459985179565
$c_2 =$	3.66869179814223
$c_3 =$	0.500703203096610
$c_4 =$	0.839359633413003
$c_5 =$	0.849965412245339
$c_6 =$	0.06550330854836428
$c_7 =$	0.3617122159967145
$c_8 =$	2.295356861354712

Table 1: The numerical values of the coefficients.

3.5 Renormalized results

We will use a renormalization scheme such that the renormalized kinetic part looks just like the classical term :

$$K_e = \frac{2}{2g_R^2} \left(c_4^a c_4^a + c_1^a c_1^a \right) ; \quad (118)$$

Using eq. (117) this gives us the finite part of the renormalization (91):

$$\frac{1}{g_R^2} = \frac{1}{g_0^2} + \frac{11}{12} \frac{1}{\epsilon} + \frac{11}{12} \frac{1}{\epsilon^2} \log\left(\frac{\mu}{2}\right) + c_0 ; \quad (119)$$

where c_0 can be found in table 1. This renormalization scheme can easily be related to other schemes like the \overline{MS} or \overline{MS} scheme.

The finite, renormalised effective potential becomes

$$V_e = \frac{2}{g_R^2} V_{cl}(c; d) + V_e^{(1)} ; \quad (120)$$

with

$$\begin{aligned} V_e^{(1)}(c; d) &= V_e^{(1)}(c) + V_e^{(1)}(d) + c_7 \text{tr}(X) \text{tr}(Y) + c_8 \text{tr}(X Y) ; \\ V_e^{(1)}(c) &= c_1 \text{tr}(X) + c_2 \det(c) + c_3 \text{tr}^2(X) + c_4 \text{tr}(X^2) \\ &\quad + c_5 \det(c) \text{tr}(X) + c_6 \text{tr}^3(X) ; \end{aligned} \quad (121)$$

with the numerical values for c_i in table 1. Note that the u^5 term in the effective potential along the tunnelling path uniquely determines the coefficient of the $\text{tr}(X) \det(c)$ term. The u^6 term can be obtained from combinations of the three independent invariants $\text{tr}^3(X)$, $\text{tr}(X) \text{tr}(X^2)$ and $\text{tr}(X^3)$. We choose to replace the u^6 term by $\text{tr}^3(X)$, which is the simplest of these from the viewpoint of the variational calculation. Note that not all of these coefficients are small, which means that the one-loop correction to the spectrum, to be calculated in section 4, may be substantial.

4 Calculating the spectrum

4.1 Introduction

In this section we will approximate the spectrum of the effective hamiltonian by applying the Rayleigh-Ritz method [29]. This is a variational method that consists of truncating some suitably chosen basis of functions and calculating the matrix of the hamiltonian H with respect to this basis. The results of the numerical diagonalization are the energy levels in various sectors. Using these, we find the excitation energies which correspond to the masses of the low-lying glueball states. We also estimate the window of validity of our effective model.

Consider a hamiltonian H whose spectrum $\sigma(H)$ is $f_1; f_2; \dots$. The Rayleigh-Ritz method gives upper bounds $\tilde{\epsilon}_n \geq \epsilon_n$. We will use the generalized Temple inequality [29, 30] to arrive at lower bounds for the levels. Let ψ be a normalized trial wave function and define

$$E = \langle \psi | H | \psi \rangle; \quad \Delta = \langle \psi | (H - E) | \psi \rangle = \langle \psi | H^2 | \psi \rangle - E^2. \quad (122)$$

Note that $\Delta \geq 0$ and that $\Delta = 0$ implies that ψ is a true eigenfunction of H . With the help of the values of $\tilde{\epsilon}_n$ we can derive lower bounds. We assume our variational basis to be so accurate that $\tilde{\epsilon}_{n+1} > (\tilde{\epsilon}_{n+1} + \tilde{\epsilon}_n)/2$. Under this and some other mild assumptions we can conclude [29, 30]

$$\tilde{\epsilon}_n - \frac{2}{\tilde{\epsilon}_{n+1} - \tilde{\epsilon}_n} < \epsilon_n < \tilde{\epsilon}_n. \quad (123)$$

We can treat the lowest order and the one-loop case on the same footing by writing

$$H = \frac{f}{2} \left(\frac{\partial^2}{\partial c_1^2 \partial c_1^2} + \frac{\partial^2}{\partial d_1^2 \partial d_1^2} \right) + V(c; d); \quad f = \frac{g^2}{2^2}; \quad (124)$$

$$V(c; d) = V(c) + V(d) + {}_7 r_c^2 r_d^2 + {}_8 \text{inv}_2(c; d); \quad (125)$$

$$V(c) = {}_1 r_c^2 + {}_2 \text{inv}_3(c) + {}_3 r_c^4 + {}_4 \text{inv}_4(c) + {}_5 r_c^2 \text{inv}_3(c) + {}_6 r_c^6; \quad (126)$$

The coefficients ${}_i$ (which are functions of f and ${}_j$) as well as the definitions of the used invariants can be found in table 2. We have also given the definitions of the invariants that occur in V^2 . For the lowest order effective hamiltonian, we just set ${}_i = 0$, whereas for the one-loop effective hamiltonian we need to use the values for ${}_i$ of table 1. A sketch of our methods and some results for the truncated model were published before [19].

4.2 The variational basis

We decided to use functions of the form $(r_c; r_d)Y(\hat{c}; \hat{d})$ and to incorporate the boundary conditions in the $(r_c; r_d)$ plane. Apart from the boundary conditions, we must also respect the symmetries of the hamiltonian as much as possible to obtain an optimal block diagonalization. Most of these symmetries, including the residual gauge symmetry, will be incorporated in the functions $Y(\hat{c}; \hat{d})$. After this, we will use the exact solution of the strong coupling limit of our hamiltonian problem as a guide to obtain a useful set of radial functions.

$1 = \frac{2}{f} + 1$		$\text{inv}_3(c) = 3 \det(c)$
$2 = \frac{2}{f} + \frac{1}{3} 2$		$\text{inv}_4(c) = \frac{1}{8} (\text{tr}^2(X) - \text{tr}(X^2))$
$3 = 3 + 4$		$\text{inv}_2(c; d) = \frac{1}{6} (\text{tr}(X) \text{tr}(Y) - \text{tr}(XY))$
$4 = \frac{2}{f} 8 4$		$\text{inv}_6(c) = \text{inv}_3^2(c)$
$5 = \frac{1}{3} 5$		$\text{inv}_7(c) = \text{inv}_3(c) \text{inv}_4(c)$
$6 = 6$		$\text{inv}_8(c) = \text{inv}_4^2(c)$
$7 = 7 + 8$		
$8 = \frac{2}{f} 6 8$		

Table 2: The coefficients for the hamiltonian and the definition of several invariants.

4.2.1 Symmetries

The hamiltonian $H(c; d)$ is invariant under the transformation $c \rightarrow S c R_1$; $d \rightarrow S d R_2$ with $S; R_1; R_2 \in SO(3)$ and under the interchange $c \leftrightarrow d$. The generators of left- and right multiplication are L_c^R, L_c^S, L_d^R and L_d^S . These are $su(2)$ angular momentum operators and we have for instance

$$L_c^R = i \epsilon_{ijk} c_j^a \frac{\partial}{\partial c_k^a} : \quad (127)$$

The following set of operators commutes:

$$H; J^S; J^R; (L_c^R)^2 + (L_d^R)^2; P : \quad (128)$$

P is defined by $P f(c; d) = f(d; c)$. On S^3 it corresponds to the parity $(n_0; \mathbf{n}) \rightarrow (n_0; -\mathbf{n})$ (cf. eq. (7)). The operator $J^S = L_c^S + L_d^S$ implements constant gauge transformations: we have to demand $(J^S)^2 = 0$ for physical wave functions. The operator $J^R = L_c^R + L_d^R$ is the rotation operator. The spatial symmetry group is $SO(4)$ and these symmetries cannot be simply divided in independent sets of translations and rotations. The operator on S^3 that corresponds to J^R is $L_1 + L_2$, and the corresponding symmetry on $SU(2)$ (cf. appendix A) is $g \rightarrow g_1^{-1} g g_1$. Writing $g = n$ and $g = n^0$ we have

$$n \rightarrow n(n^0)^{-1}(n^0) = n_0^{-1} n_i V_i^j (n^0)^j : \quad (129)$$

The symmetry on S^3 is thus seen to leave n_0 invariant and to perform an $SO(3)$ rotation on \mathbf{n} . It is hence a rotation for points around the north and south pole of S^3 . The operators L_1 and L_2 do not leave any point invariant and cannot be interpreted as rotation operators. Only their sum has this property and the different sectors ($j = 0; 1; \dots$) under the symmetry J^R correspond to scalar glueballs, vector glueballs, etc.

To prepare the ground for the block diagonalization of the hamiltonian, we divide the function space in sectors characterized by the quantum numbers $j, m, l_1(l_1 + 1) + l_2(l_2 + 1)$ and p corresponding to the operators of eq. (128). Note that for low values of l_1 and l_2 there is a one-to-one correspondence between unordered pairs $(l_1; l_2)$ and the numbers $l_1(l_1 + 1) + l_2(l_2 + 1)$. Since the spectrum of H is independent of the azimuthal quantum number m , we use the notation $l_1 l_2$ j -even and $l_1 l_2$ j -odd to denote the various sectors. The lowest energy level in the scalar ($j = 0$) sector is the vacuum. Energy differences with respect to this level will be the glueball masses.

Operator	$(\mathbb{L}_c^S)^2$	$(\mathbb{L}_c^S)_3$	$(\mathbb{L}_c^R)^2$	$(\mathbb{L}_c^R)_3$	\hat{c}
Eigenvalue	$l_s(l_s + 1)$	m_s	$l_r(l_r + 1)$	m_r	$L(L + 7)$

Table 3: Behaviour of the functions $h\hat{\mathcal{J}}; l_s; l_r; m_s; m_r i$.

4.2.2 The angular sector

We begin with constructing functions of \hat{c} that are eigenfunctions of the following set of commuting operators

$$n_{\hat{c}}; \mathbb{L}_c^R; \mathbb{L}_c^S : \quad (130)$$

Note that the space of the \hat{c} makes up an S^8 . From appendix A we know that the eigenfunctions of the spherical laplacian $\Delta_{\hat{c}}$ will be the homogeneous harmonic polynomials in \hat{c} . An orthonormal basis of functions of \hat{c} is given by the set $fh\hat{\mathcal{J}}; l_s; l_r; m_s; m_r i$. Each of these functions is a homogeneous harmonic polynomial of degree L in \hat{c} . Its eigenvalues under the various symmetries are collected in table 3. We used the operators \mathbb{L}_c^R and \mathbb{L}_c^S to further classify these functions, but for higher values of L we need the extra label ℓ for the remaining degeneracy. This degeneracy is absent for low values of L , shows up first for $(L; l_s; l_r) = (4; 2; 2)$ and proliferates for high values of L .

Explicitly, we have that $h\hat{\mathcal{J}}; 0; 0; 1; 0; 0 i$ is just the constant function. For $L = 1$ we have the nine functions c_1^a . With the help of the raising and lowering operators L^S and L^R we arrive at the nine functions $h\hat{\mathcal{J}}; 1; 1; 1; m_s; m_r i$ which are the appropriate complex linear combinations $fc_+^+; c_+^0; c_+; c_0^+; c_0^0; c_0^-; c_-; c_-^0; c_-^+$ of the variables c_1^a . We have e.g. $L_3^S c_+ = c_+$ and $L_3^R c_+ = c_+$.

To construct all representations $(L; l_s; l_r; \ell)$ for given $(L; l_s; l_r)$, we proceed as follows. We construct the eigenspace $A_{l_r}^{l_s}$ of the operators L_3^S and L_3^R . This is the space span by all monomials of degree L in the complex c variables that have the eigenvalues l_s and l_r under the operators L_3^S and L_3^R . Within $A_{l_r}^{l_s}$, but now regarded as functions of c instead of \hat{c} , we construct the intersection of the kernels of the operators $L^S L_+^S, L^R L_+^R$ and $(c_1^a c_1^a)$. The first two operators leave us with only those combinations of the monomials that have the prescribed $(\mathbb{L}^S)^2$ and $(\mathbb{L}^R)^2$ eigenvalues; the laplacian imposes the constraint that the polynomials must be harmonic: $\Delta_{\hat{c}} = 0$. If this intersection consists of more than one function, we use explicit Gram-Schmidt orthogonalization to arrive at the functions $h\hat{\mathcal{J}}; l_s; l_r; \ell; l_r i$. With the lowering operators, we trivially construct the rest of the functions $h\hat{\mathcal{J}}; l_s; l_r; \ell; m_s; m_r i$.

Most calculations were done in MATHEMATICA, but we used C to perform the construction of the intersection of the kernels of $L^S L_+^S$ and $L^R L_+^R$. For this we used the explicit projectors on the kernel

$$P_{l_s}^S = \prod_{j=l_s+1}^{l_s} \mathbb{1} - \frac{1}{j(j+1) - l_s(l_s+1)} L^S L_+^S ; \quad (131)$$

and the analogous expression for $P_{l_r}^R$. Since all calculations had to be done exactly, we used arithmetic with (large) integers. In this way we explicitly constructed the representations

Operator	$(\mathbb{L}_c^S)^2$	$(\mathbb{L}_d^S)^2$	$(\mathbb{J}^S)^2$	\mathbb{J}_3^S	\hat{c}
Eigenvalue	$\mathbb{l}_s(\mathbb{l}_s + 1)$	$\mathbb{l}_s(\mathbb{l}_s + 1)$	0	0	$\mathbb{L}_1(\mathbb{L}_1 + 7)$

Operator	$(\mathbb{L}_c^R)^2$	$(\mathbb{L}_d^R)^2$	$(\mathbb{J}^R)^2$	\mathbb{J}_3^R	\hat{d}
Eigenvalue	$\mathbb{l}_1(\mathbb{l}_1 + 1)$	$\mathbb{l}_2(\mathbb{l}_2 + 1)$	$\mathbb{j}(\mathbb{j} + 1)$	\mathbb{m}	$\mathbb{L}_2(\mathbb{L}_2 + 7)$

Table 4: Behaviour of the functions $h\hat{c}\hat{j};m;\mathbb{l}_s;\mathbb{L}_1;\mathbb{l}_1;\mathbb{l}_2;\mathbb{L}_2;\mathbb{l}_2;\mathbb{j};\mathbb{m}$.

$(\mathbb{L};\mathbb{l}_s;\mathbb{l}_r;)$ for $\mathbb{L} = 10$ and $\mathbb{l}_r = 2$. As will be apparent from the sequel, we did not need higher values for \mathbb{l}_r .

We construct functions of both \hat{c} and \hat{d} by using the familiar rules of adding angular momenta. Let i denote a representation $(\mathbb{L};\mathbb{l}_s;\mathbb{l}_r;)$ and consider the functions $h\hat{c}\hat{j};m_s;m_r$ and $h\hat{d}\hat{j};m_s^0;m_r^0$. Using Clebsch-Gordan coefficients, we can define a function $Y^{\mathbb{l}_1\mathbb{l}_2}(\hat{c};\hat{d})$ which is an eigenfunction of \mathbb{J}^R and of \mathbb{J}^S . We will limit the construction to functions with $\mathbb{J}^S = 0$, as required by residual gauge symmetry. This implies that the functions of c and d need to have the same \mathbb{l}_s , which restricts the possible combinations of \mathbb{l}_1 and \mathbb{l}_2 . The resulting function is given by

$$\begin{aligned}
Y^{\mathbb{l}_1\mathbb{l}_2}(\hat{c};\hat{d}) &= h\hat{c}\hat{j};m;\mathbb{l}_s;\mathbb{L}_1;\mathbb{l}_1;\mathbb{l}_2;\mathbb{L}_2;\mathbb{l}_2;\mathbb{j};\mathbb{m} \\
&= \sum_{m_s=\mathbb{l}_s} \sum_{m_1=\mathbb{l}_1} \sum_{m_2=\mathbb{l}_2} \frac{(-1)^{\mathbb{l}_1-\mathbb{l}_2+m}}{(2\mathbb{j}+1)} \frac{0}{2\mathbb{j}+1} \frac{1}{\mathbb{A}} \\
&\quad \frac{(-1)^{\mathbb{l}_s-m_s}}{(2\mathbb{l}_s+1)} h\hat{c}\hat{j}_1;\mathbb{l}_s;\mathbb{l}_1;\mathbb{m}_s;\mathbb{m}_1; h\hat{d}\hat{j}_2;\mathbb{l}_s;\mathbb{l}_2;\mathbb{m}_s;\mathbb{m}_2; \quad (132)
\end{aligned}$$

Its eigenvalues under the various symmetries are collected in table 4. Note the behaviour under parity:

$$P Y^{\mathbb{l}_1\mathbb{l}_2} = (-1)^{\mathbb{l}_1+\mathbb{l}_2+\mathbb{j}} Y^{\mathbb{l}_2\mathbb{l}_1}; \quad (133)$$

4.2.3 The radial sector

The strong coupling limit of our hamiltonian problem consists of the eigenvalue problem for the kinetic part of the hamiltonian of eq. (49). If we assume a solution $'(r_c)'(r_d)Y^{\mathbb{l}_1\mathbb{l}_2}(\hat{c};\hat{d})$, the reduced one-dimensional eigenvalue problem becomes

$$\frac{\partial^2}{\partial r^2} + \frac{(12 + \mathbb{L}(\mathbb{L} + 7))}{r^2} ' (r) = 0; \quad (134)$$

whose regular solution is $'^{(\mathbb{L})}(r) = r \mathbb{j}_{\mathbb{L}+1}(r)$, with $\mathbb{j}_p(z)$ the spherical Bessel function of order p and $\mathbb{L} = \mathbb{l}_1 + \mathbb{l}_2$. The eigenfunctions of the kinetic part of the hamiltonian are thus given by

$$'_{\mathbb{l}_1}^{(\mathbb{L}_1)}(r_c)'_{\mathbb{l}_2}^{(\mathbb{L}_2)}(r_d)Y^{\mathbb{l}_1\mathbb{l}_2}(\hat{c};\hat{d}); \quad (135)$$

with the energies given by $E = \frac{f}{2}(\frac{\mathbb{l}_1}{2} + \frac{\mathbb{l}_2}{2})$.

During the variational stage of the calculation, however, the use of spherical Bessel functions of different order will lead to a large number of integrals. Therefore we take the radial functions to be independent of L_1 and L_2 and define

$$\psi_{12}^{i_1 i_2}(c; d) = j_{l_1}^{i_1}(r_c) j_{l_2}^{i_2}(r_d) Y_{l_1 l_2}^{i_1 i_2}(\hat{c}; \hat{d}); \quad (136)$$

with $j_l(r) = r^{-l} j_l(r)$. These functions are not eigenfunctions of the kinetic part of the hamiltonian and they will have discontinuities of the following kind. For $r \neq 0$, we have that $j_l(r) \sim r^l$. The wave function behaves as $r^{-l_1 - l_2} \psi_{12}^{i_1 i_2}(c; d)$, and this function will be discontinuous at $r = 0$. The variational functions thus have discontinuities at $r_c = 0$ and $r_d = 0$. These discontinuities form a set of measure zero, and a variational calculation will not feel them. Since the functions $j_l(r)$ are the eigenfunctions of the reduced one-dimensional problem with $L = 0$, they still constitute a complete set of functions.

The behaviour under parity can be obtained from eq. (133) and is given by

$$P \psi_{12}^{i_1 i_2} = (-1)^{l_1 + l_2 + j} \psi_{21}^{i_2 i_1}; \quad (137)$$

Taking even and odd combinations gives

$$P \psi_{12}^{i_1 i_2}(c; d) = \psi_{12}^{i_1 i_2}(c; d) + p \psi_{12}^{i_1 i_2}(d; c); \quad (138)$$

We implement the boundary conditions eq. (57) and (58) for $\theta = 0$ by imposing the following conditions on ψ_1 and ψ_2 :

$$p = -1 : \psi_1(\frac{\pi}{3}) = \psi_2(\frac{\pi}{3}) = 0; \quad (139)$$

$$p = 1 : \frac{\partial(r^{\frac{5}{2} - l_1})}{\partial r} \psi_1(\frac{\pi}{3}) = \frac{\partial(r^{\frac{5}{2} - l_2})}{\partial r} \psi_2(\frac{\pi}{3}) = 0; \quad (140)$$

These conditions are expected to be accurate as long as the wave function transverse to the sphaleron path (near the sphalerons) is predominantly in its ground state. The case $\theta = \pi$ can be treated along the same lines as $\theta = 0$ by interchanging the boundary conditions for the cases $p = 1$ and $p = -1$.

The exact strong coupling results for the lowest levels in some sectors for $\theta = 0$ are collected in table 5. These values are obtained by imposing the boundary conditions above on the true eigenfunctions of eq. (135): the values of ψ_1 and ψ_2 are hence dependent on L_1 and L_2 respectively.

For general θ we multiply $\psi_{12}^{i_1 i_2}(c; d)$ with a phase factor $\exp(i \theta(r_c; r_d))$. The function is a kind of Chern-Simons functional that gives the correct behaviour to the wave function under large gauge transformations. The resulting functions no longer have well-defined parity, but they do obey the general boundary conditions for suitable θ . Also the hermiticity of the hamiltonian for these functions can be checked explicitly. Sufficient conditions on θ are: $\theta(r_c; r_d) = \theta(r_d; r_c)$ and $\theta(\frac{\pi}{3}; 0) = \frac{1}{2}$. We choose

$$\theta(r_c; r_d) = \frac{1}{2} \theta \left(\frac{r_c}{\frac{\pi}{3}}, \frac{r_d}{\frac{\pi}{3}} \right) : \quad (141)$$

For $\theta \rightarrow 1$ we approach the situation that the phase factor over the entire edge is constant and equal to e^i . But already for the choice $\theta = 2$, the boundary conditions at the sphalerons are taken into account properly.

sector	$j; m; l_s; L_1; l_1; L_2; l_2; i$	1	2	E
000-even	$0; 0; 0; 0; 0; 1; 0; 0; 1i$	1.9786	1.9786	3.9149f
000-even	$0; 0; 0; 0; 0; 1; 3; 0; 1i$	1.9786	4.1215	10.4508f
000-odd	$0; 0; 0; 0; 0; 1; 0; 0; 1i$	4.0345	6.0143	26.2246f
112-even	$2; m; 1; 1; 1; 1; 1; 1; 1i$	2.7406	2.7406	7.5108f
112-odd	$2; m; 1; 1; 1; 1; 2; 1; 1i$	4.7242	5.4016	25.7476f
022-even	$2; m; 0; 0; 0; 1; 2; 2; 1i$	1.9786	3.4456	7.8936f
022-odd	$2; m; 0; 0; 0; 1; 2; 2; 1i$	4.0345	5.4016	22.7272f

Table 5: Strong coupling limit: lowest energy levels in some sectors.

4.3 Matrix elements

In this section we will describe the calculation of the matrix elements of H and of H^2 . The hamiltonian $H = K + V$ is given by eq. (49). We let $j|i$ denote the normalized basis function:

$$j|i / \sqrt{\frac{i_1 i_2}{1! 2!}} (c; d) + p(1)^{l_1 + l_2 + j} \sqrt{\frac{i_2 i_1}{2! 1!}} (c; d) \exp(i(r_c; r_d)); \quad (142)$$

with $\sqrt{\frac{i_1 i_2}{1! 2!}} (c; d)$ given by eq. (136). We take from eq. (141) with $\ell = 2$: $(r_c; r_d) = \frac{1}{6} (r_c^2 - r_d^2)$.

Consider first the matrix element $\langle n^0 | H | j|i \rangle$. For the potential energy V the phase factor $\exp(i(r_c; r_d))$ cancels against its complex conjugate. For the kinetic operator we obtain

$$\begin{aligned} \exp(-i(r_c; r_d)) K \sqrt{\frac{i_1 i_2}{1! 2!}} (c; d) \exp(i(r_c; r_d)) = \\ \frac{f}{2} \left(\frac{2}{1} + \frac{2}{2} + \frac{L_1(L_1 + 7)}{r_c^2} + \frac{L_2(L_2 + 7)}{r_d^2} \right) \sqrt{\frac{i_1 i_2}{1! 2!}} (c; d) \\ + \frac{f}{2} \left(i \frac{2}{3} r_c \frac{\partial'_{-1}(r_c)}{\partial r_c}, \frac{\partial'_{-2}(r_d)}{\partial r_d} - \frac{\partial'_{-1}(r_c)}{\partial r_c} r_d \frac{\partial'_{-2}(r_d)}{\partial r_d} \right) Y^{i_1 i_2}(\hat{c}; \hat{d}) \\ + \frac{f}{2} \left(\frac{2}{9} (r_c^2 + r_d^2) \right)'_{-1}(r_c)'_{-2}(r_d) Y^{i_1 i_2}(\hat{c}; \hat{d}); \end{aligned} \quad (143)$$

To apply Temple's inequality, we need the matrix elements of H^2 . Using the hermiticity of H we write

$$\begin{aligned} \langle n^0 | H^2 | j|i \rangle &= \langle n^0 | (K + V) n^0 | j(K + V) | n^0 \rangle \\ &= \frac{1}{2} \langle n^0 | K n^0 | j(K + V) | n^0 \rangle + \frac{1}{2} \langle n^0 | V^2 | j|i \rangle + \text{hermitian conjugate}; \end{aligned} \quad (144)$$

From these expressions we can read off which matrix elements we have to calculate.

Since the potential $V(c; d)$ is invariant under \mathcal{L}_c^R and \mathcal{L}_d^R as well as under \mathcal{J}^S , all the terms in V and V^2 are of the form

$$A = \langle \hat{c} \hat{d} | 0; 0; l_s; L_1; 0; \gamma_1; L_2; 0; \gamma_2 | i; \quad (145)$$

By virtue of the construction in eq. (132) all the angular integrations over \hat{c} and \hat{d} can be reduced to angular integrations in R^9 . These integrals can be expressed in terms of reduced matrix elements. The details on this procedure can be found in appendix C.

The radial integrals we need to compute are

$$J(n; 0;) = \int_0^{z/\sqrt{3}} dr r^n \hat{c}_0(r) \hat{c}_0(r); \quad (146)$$

$$J_1(n; 0;) = \int_0^{z/\sqrt{3}} dr r^n \hat{c}_0(r) r \frac{\partial}{\partial r} \hat{c}_0(r); \quad (147)$$

$$J_{11}(n; 0;) = \int_0^{z/\sqrt{3}} dr r^n r \frac{\partial}{\partial r} \hat{c}_0(r) r \frac{\partial}{\partial r} \hat{c}_0(r); \quad (148)$$

where \hat{c}_0 is normalized to one, and

$$\hat{c}_0(r) = r j_0(r) = f(z); \quad (149)$$

$$f(z) = 1 - \frac{15}{z^2} \cos(z) + \frac{6}{z} + \frac{15}{z^3} \sin(z); \quad (150)$$

Consider the integral for non-normalized f functions and let $z = \frac{p}{\sqrt{3}}$ and $0 = \frac{p}{\sqrt{3}} 0$. For an explicit value of n , but unspecified values of 0 and z , we write

$$\mathcal{J}(n) = \int_0^{z/\sqrt{3}} dr r^n f_0(r) f_0(r) = \left(\frac{p}{\sqrt{3}}\right)^{n+1} \int_0^z dx x^n f_0(x) f_0(x); \quad (151)$$

We express products of sines and cosines of x and $0x$ in sines and cosines of sx and vx with $s = 0 +$ and $v = 0$. The integrand as it stands is regular at $x = 0$, but individual terms need not be. We therefore introduce a cut-off ϵ , after which the integral is a sum of functions

$$\cos(m; a) = \int_{\epsilon}^{z/\sqrt{3}} dx x^m \cos(ax); \quad \sin(m; a) = \int_{\epsilon}^{z/\sqrt{3}} dx x^m \sin(ax); \quad (152)$$

Using recursion formulae obtained from partial integration allows us to eliminate the functions $\cos(m; a)$ and $\sin(m; a)$. After taking the limit $\epsilon \rightarrow 0$, the result is an expression in the functions \sin , \cos , Si , Ci and \ln of the variables s and v . By substituting values for s and v and performing the normalization we construct tables for $J(n; 0;)$. Note that we have to be careful for $0 =$: we have to take the limit $v \rightarrow 0$ before substituting actual values.

The other integrals $J_1(n)$ and $J_{11}(n)$ can be obtained as follows:

$$\begin{aligned} J_1(n) &= \int_0^{z/\sqrt{3}} dr r^n f_0(r) r \frac{\partial}{\partial r} f_0(r) \\ &= \left(\frac{p}{\sqrt{3}}\right)^{n+1} \int_0^z dx x^n f_0(x) x \frac{\partial}{\partial x} f_0(x) \\ &= \frac{\partial}{\partial z} \mathcal{J}(n) \\ &= \frac{s-v}{2} \frac{\partial}{\partial s} \frac{\partial}{\partial v} \mathcal{J}(n); \end{aligned} \quad (153)$$

4.4 Weak coupling expansion

In this section we will perform the perturbative calculation of the energy levels of the hamiltonian. The results will serve as a check on the variational calculation in the regime of small coupling constant. Starting from the strong coupling basis, we could also develop a perturbation theory in $\frac{1}{f}$, but there are two reasons why this is less interesting. First, we are interested in the region where we just start to see the deviations from perturbative behaviour in f . Second, since our variational basis is in essence a strong coupling basis, the reproduction of the strong coupling limit does not give a strong check on the variational calculation.

For the weak coupling limit, we rescale $x_c = \sqrt{\frac{q}{f}} r_c$ and $x_d = \sqrt{\frac{q}{f}} r_d$ and we split the hamiltonian of eq. (49) in $H = H_0 + H_1$, with

$$H_0 = \frac{\partial^2}{\partial x_c^2} + \frac{\partial^2}{\partial x_d^2} + 12 \left(\frac{1}{x_c^2} + \frac{1}{x_d^2} \right) + \frac{1}{x_c^2} c + \frac{1}{x_d^2} d + x_c^2 + x_d^2; \quad (154)$$

$$H_1(c;d) = H_1(c) + H_1(d) + \frac{f}{2} x_c^2 x_d^2 + \frac{f}{2} x_c^2 x_d^2 \text{inv}_2(\hat{c};\hat{d}); \quad (155)$$

$$\begin{aligned} H_1(c) = & \frac{f}{2} x_c^2 + \frac{f}{2} x_c^3 \text{inv}_3(\hat{c}) + \frac{f}{2} x_c^4 \\ & + \frac{f}{2} x_c^4 \text{inv}_4(\hat{c}) + \frac{f}{2} x_c^5 \text{inv}_5(\hat{c}) + \frac{f}{2} x_c^6; \end{aligned} \quad (156)$$

Diagonalizing H_0 leads to the following one-dimensional eigenvalue problem :

$$\frac{\partial^2}{\partial x^2} + \frac{12 + L(L+7)}{x^2} \psi(x) = 0; \quad (157)$$

The regular solution of this equation is [31]

$$\psi(x) = e^{-\frac{1}{2}x^2} x^{L+4} {}_1F_1\left(-\frac{2L+9}{4}; L+\frac{9}{2}; x^2\right); \quad (158)$$

with ${}_1F_1$ the confluent hypergeometric function. As in the strong coupling case, we can use the boundary conditions at $x = \sqrt{\frac{6}{f}}$ to discretize the possible values for L and hence the energy. This would give us an alternative to the strong coupling basis constructed earlier. Disadvantages of this basis are that the functions themselves depend on the coupling constant f . Also the matrix elements of operators between two confluent hypergeometric functions are hard to calculate. For the variational method, we will therefore use the strong coupling basis.

We can however use the weak coupling basis for perturbation purposes. For $f \neq 0$ the location where the boundary conditions have to be imposed moves away to infinity, which is equivalent to saying that the wave function, in the original coordinates, is strongly localized around $c = d = 0$. We can replace the boundary conditions at $x = \sqrt{\frac{6}{f}}$ by demanding normalizability of the functions $\psi(x)$. This means that the ${}_1F_1$ function must reduce to a polynomial, which is the case if its first argument is $-n$ with $n = 0; 1; \dots$. The ${}_1F_1$ function then reduces to a Laguerre polynomial and we obtain the discretization $L = 9 + 2L + 4n$. The weak coupling eigenfunctions are thus

$$\psi_{n_1 n_2} = L_{n_1}^{(L_1 + \frac{7}{2})}(x_c^2) L_{n_2}^{(L_2 + \frac{7}{2})}(x_d^2) x_c^{(L_1+4)} x_d^{(L_2+4)} e^{-\frac{1}{2}x_c^2} e^{-\frac{1}{2}x_d^2} Y_{i_1 i_2}(\hat{c};\hat{d}); \quad (159)$$

and the energies are given by

$$E = 18 + 2(L_1 + L_2) + 4(n_1 + n_2): \quad (160)$$

We use Bloch's formulation [25, 1] of perturbation theory to calculate the weak coupling expansion of the energy levels of the hamiltonian. For this we need the matrix elements of H_I w.r.t. the basis of eq. (159). The angular integrations are treated in appendix C. The radial integrals take the form

$$\int_0^1 dx x^n e^{-x^2} x^{L_0+4} x^{L_1+4} L_{n_0}^{(L_0+\frac{7}{2})}(x^2) L_{n_1}^{(L_1+\frac{7}{2})}(x^2): \quad (161)$$

We calculate these integrals by substituting the explicit form of the Laguerre polynomials.

Using orthogonality properties of the Laguerre polynomials and of the angular functions, one can show that the number of intermediate levels that we have to take into account is finite. To be more precise: given the values E and L for an unperturbed level and the requested accuracy in terms of powers of the coupling constant, one can calculate maximum values E_{max} and L_{max} beyond which there will be no contribution up to the requested accuracy.

We will give the perturbative results for those levels which will turn out to correspond to the lowest glueball masses:

$$E_{000\text{-even}}^{(0)} = 18 + f \left[\frac{9}{8} + \frac{9}{2} \epsilon_1 \right] + f^2 \left[\frac{63}{512} - \frac{9}{16} \epsilon_1^2 - \frac{3}{8} \epsilon_2 \right] + \frac{99}{8} \epsilon_3 + \frac{63}{8} \epsilon_4 + \frac{81}{16} \epsilon_7 + \frac{27}{16} \epsilon_8 + O(f^3); \quad (162)$$

$$E_{000\text{-even}}^{(1)} = 22 + f \left[\frac{9}{8} + \frac{11}{2} \epsilon_1 \right] + f^2 \left[\frac{903}{512} + 3 \epsilon_1 - \frac{11}{16} \epsilon_1^2 - \frac{13}{8} \epsilon_2 \right] + \frac{165}{8} \epsilon_3 + \frac{105}{8} \epsilon_4 + \frac{135}{16} \epsilon_7 + \frac{45}{16} \epsilon_8 + O(f^3); \quad (163)$$

$$E_{000\text{-odd}}^{(0)} = 22 + f \left[\frac{13}{8} + \frac{11}{2} \epsilon_1 \right] + f^2 \left[\frac{1063}{512} + \frac{13}{4} \epsilon_1 - \frac{11}{16} \epsilon_1^2 - \frac{13}{8} \epsilon_2 \right] + \frac{165}{8} \epsilon_3 + \frac{105}{8} \epsilon_4 + \frac{99}{16} \epsilon_7 + \frac{33}{16} \epsilon_8 + O(f^3); \quad (164)$$

$$E_{112\text{-even}}^{(0)} = 22 + f \left[\frac{13}{24} + \frac{11}{2} \epsilon_1 \right] + f^2 \left[\frac{3167}{4608} + \frac{25}{24} \epsilon_1 - \frac{11}{16} \epsilon_1^2 - \frac{7}{8} \epsilon_2 \right] + \frac{143}{8} \epsilon_3 + \frac{91}{8} \epsilon_4 + \frac{121}{16} \epsilon_7 + \frac{47}{16} \epsilon_8 + O(f^3); \quad (165)$$

4.5 Results

With the results of the previous sections, we are in a position to actually perform the variational calculation. A FORTRAN programme constructed the truncated matrix for the hamiltonian and performed the diagonalization using routines from the Nag-library and the Eispack library. The output consisted of the upper bounds $\tilde{\epsilon}_n$ for the lowest energy eigenvalues and of the corresponding values for ϵ_n (used for computing lower bounds). We also produced graphical representations of the wave function. These can be used in verifying a posteriori whether the assumption is true that the boundary conditions are only felt at or near the sphalerons.

4.5.1 Low est-order ham iltonian

We start by considering the lowest order results. After calculating the lowest levels in various sectors, we find that the lowest glueball masses are to be found in the sectors 000-even, 000-odd and 112-even for respectively the scalar and the tensor glueballs. These levels, including the lower bounds and the perturbative expansions, are plotted in fig. 3. Note that the crossing of levels only happens for levels that are in different sectors. States within the same sector would exhibit avoided level crossing due to level repulsion.

For small coupling, the deviations of the wave function from the perturbative one will be small. To reproduce the energy eigenvalues correctly, we can suffice with a relatively low number of angular functions, but to be able to accommodate the strong localization around $c = d = 0$, we need a large number of radial functions. For larger values of f we can reduce the number of radial functions, but we must increase the number of angular functions. The data we used was obtained by combining different runs with various choices for the truncated basis as controlled by the parameters N_{rad} (number of radial functions) and L_{sum} (limit on $L_1 + L_2$).

In the 000-even sector we maximally used $N_{\text{rad}} = 150$ and $L_{\text{sum}} = 10$ for small f , and $N_{\text{rad}} = 50$ and $L_{\text{sum}} = 14$ for larger values of f . These values correspond to bases consisting of over 3000 vectors. Increasing the number of basis vectors becomes quickly limited by the amount of free memory available in the computer. For the case $\epsilon \neq 0$, the hamiltonian is complex and we need a factor of two more memory. In the 112-even sector, the same number for L_{sum} resulted in higher numbers of angular functions. Here we went up to $N_{\text{rad}} = 150$ and $L_{\text{sum}} = 8$ for small f , and $N_{\text{rad}} = 30$ and $L_{\text{sum}} = 12$ for larger values of f .

We did most of the calculations on Sun workstations. For some values of f we wanted more accurate results and used computer time on a Cray. We also developed a pruning technique: after diagonalization, we examine the variational wave function obtained for, say, the ground state. We replace those basis vectors (roughly ten to twenty percent) that have a small coefficient in this wave function by new basis vectors and repeat the diagonalization. Repeating this procedure allows us to sample a larger variational basis, but we do not have the guarantee that the results will improve in this way: it is possible that the true wave function has substantial overlap with very many vectors in our basis.

Returning to our calculation, the lowest-lying scalar ($j = 0$) and tensor ($j = 2$) levels are found in respectively the sectors 000 and 112. For $\epsilon = 0$, the vacuum corresponds to the ground state of the 000-even sector. The scalar glueball 0^+ can be identified with the first excited state in the 000-even sector, the tensor glueball 2^+ with the ground state in the 112-even sector. Note that at $f = 0.6$ these levels cross, thus making the scalar glueball heavier than the tensor. We do, however, not expect our model to be valid anymore for these values of the coupling constant. Taking differences of the energy levels with respect to the ground state in the 000-even sector gives us the masses of the low-lying glueball states (fig. 4). To check on the strong coupling results, we also performed variational calculations for large values of f . The comparison with the results of table 5 can be seen in fig. 5.

For small f , there is virtually no dependence of the masses on ϵ , whereas for larger f the dependence becomes bigger. This is shown in fig. 6. For $\epsilon = 0$ we can impose the boundary conditions exactly, that is, without using the trick with the Chem-Simons like operator, but with the same method that we imposed the $\epsilon = 0$ conditions. The

variational results obtained in this way are also plotted in g. 6. Remember that a dependence is a sign that the boundary in the $(r_c; r_d)$ plane is felt. Our model is valid for values of the coupling constant at which only the boundary conditions at and near the sphalerons are felt. Checking this a posteriori with the help of plots of the wave function (g. 7) indicates that f should not be larger than roughly 0.5. These plots were obtained as follows. Consider the function

$$j(r_c; r_d)^2 = \int d\hat{c} d\hat{d} j(c; d)^2; \quad (166)$$

which is a measure of the probability distribution in the $(r_c; r_d)$ plane. Dividing this $j(r_c; r_d)$ by $r_c^4 r_d^4$, we obtain a function with the expected behaviour of the true wave function: it is localized at the sphalerons and decays exponentially in the transverse directions (see g. 7). Note that the characteristic width grows with increasing f . Although the lowest barrier is the sphaleron, the measure factor $r_c^4 r_d^4$ causes the configurations that are close to the sphaleron but have a somewhat higher energy to make the dominant contribution to the tunnelling. The relevant parameter here is the characteristic decay length of the wave function, which in turn is determined by the rise of the potential in the transverse directions.

Although we are primarily interested in the case $\epsilon = 0$, an appreciable dependence on f for a certain value of f shows that the non-perturbative influence of the boundary has become important. To explain the fact that the spectrum is not exactly periodic in f , note that our implementation of the ϵ dependence (eq. (141)) only has this periodicity in the limit $\epsilon \rightarrow 1$. The volume effect described above implies that the relevant distribution $j(r_c; r_d)$ samples a piece of the boundary over which the phase difference already starts to depart from e^i . This also implies that the results using the exact implementation of the boundary conditions for the case $\epsilon = 0$ can be expected to differ from those using the method of eq. (141). Increasing ϵ would improve the periodicity properties, but would not result in a better effective model: although it would be less apparent, the wave function would still be spread out over the boundary.

4.5.2 One-loop hamiltonian

We present basically the same plots for the one-loop hamiltonian as for the lowest order hamiltonian. As before, the lowest glueball masses are to be found in the sectors 000-even, 000-odd and 112-even. These levels, including the lower bounds and the perturbative expansions, are plotted in g. 8. Note the avoidance of level crossing between the ground state and the first excited state in the 000-even sector, which gives rise (cf. eq. (123)) to relative large errors for even the ground state.

Especially in the 112-even sector, the values obtained for ϵ are rather large. We like to stress here that the lower bounds as obtained by Temple's inequality are rather conservative and that the actual error is often much smaller. This insight is gained in studying toy models, but the effect can also be observed in the case at hand. Going from $L_{\text{sum}} = 12$ to $L_{\text{sum}} = 14$ in the 112-even sector, the upper bounds shifted very little, whereas a reduction of the ϵ value by a factor of two was achieved.

It is to be expected that for the one-loop hamiltonian a larger number of basis vectors is required, since the potential has a more complicated structure in this case. Also the values

of the coefficients in the potential may cause the large values of β . When investigating the influence of β_1 on the variational results, we find that the large value of β_8 seems to cause the problems. This coefficient corresponds to the operator $\text{inv}_2(c;d)$ (see eq. (125) and table 2), which is the only operator in the potential that can change the L_5 value of a basis function. Apparently, our basis could not be chosen so large as to yield high-precision results when the coefficient of this operator becomes large.

Taking differences of the energy levels with respect to the ground state in the 000-even sector again gives us the masses of the low-lying glueball states: see g. 9. Fig. 10 shows the dependence of the scalar glueball. In view of the remarks above, we left out the lower bounds in these cases. We can again study the localization properties around the sphaleron: see g. 11.

4.5.3 Discussion

Using the Rayleigh-Ritz method we can determine the spectrum of the effective hamiltonians. The use of Temple's inequality gives us confidence that our results are accurate, especially since experience tells us that the actual error is usually much smaller than the conservative estimates based on the values of β . The results are also consistent with the strong coupling limit and with the weak coupling perturbative expansion.

Let us focus first on small values of f . Here the boundary conditions are not felt yet, and the variational results are in accordance with the results from perturbation theory. When f grows, we see the effect of the boundary conditions in field space set in. For even larger f , the wave function has spread out over the entire $(r_c; r_d)$ plane, and the model has lost its validity. It is however possible that this already happens before this point because of a break down of the adiabatic approximation. In order for the adiabatic approximation to be valid, the wave function for the transverse modes must still be in its ground state. To check this for the modes outside the $(c;d)$ space is hard, but transverse to the tunneling path we can examine the transverse modes within the $(c;d)$ space. Fig. 7 and 11 do not only show the localization of the transverse wave function at the sphaleron, but also indicate that this transverse wave function is in its ground state. We therefore assume that the adiabatic approximation is valid, and that values of the coupling constants for which our effective model is useful are determined by the spreading out over the $(r_c; r_d)$ plane.

From these considerations, we derive the following windows in the coupling constant. For the lowest order hamiltonian, the interesting window is between $f = 0.3$ and $f = 0.5$. For the one-loop case, it is between $f = 0.2$ and $f = 0.3$.

One of the issues raised above was the level of localization of the wave function around the sphaleron. This is related to the assumption that only the boundary conditions at and near the sphalerons are felt. We argued that this was determined by the rise of the potential in the transverse directions. The one-loop correction to the $\text{tr}(Y)$ term in the potential at the c sphaleron, which can be expressed in β_1 , β_7 and β_8 , is such that it results in a lesser degree of localization. In both the lowest order and the one-loop case, a strong localization of the wave function around the sphaleron is not realized and the boundary conditions are not felt exclusively at the sphalerons. This should not come as a big surprise since it is unnatural for an eigenvalue problem that the spectrum is determined by boundary conditions at a finite number of points. Typically the conditions at a boundary with codimension one determine the spectrum. This is illustrated by our problem: we feel the

conditions at a finite part of the boundary, determined by the localization potential in the transverse directions. As long as the coupling is low enough, our assumption that the boundary conditions are only felt close to the sphalerons is true and the results are valid.

5 Conclusions

The goal of this project was to calculate the glueball spectrum on S^3 . In particular, we set out to study the effects of the topology of the configuration space on the spectroscopy. These effects can be seen as the result of the presence of instantons.

It is important to emphasize one should not expect our results for the spectrum to be accurate for large volumes. For large volumes the effects of the non-trivial topology and geometry (curvature of the configuration space, not to be confused with the curvature of S^3) become too strong to be described by the effective theory. Within the effective theory we clearly observe that at large coupling the wave functional will start to feel more of the boundary of the fundamental domain than just the neighbourhood of the sphaleron. However, it has been the main aim of this study to demonstrate that instanton effects on the low-lying spectrum are large, but calculable as long as energies remain close to the sphaleron energy, where nevertheless semiclassical techniques will completely fail.

The fact that $m_{0^+} R$ is decreasing, down from $m_{0^+} R = 4$, is what should be expected for the following reason. A rough estimate for where one would expect instantons to become relevant, based on what one finds on T^3 , would be $m_{0^+} R \approx 1.4$. Here we equate the largest geodesic distance on a torus of size L , $\frac{2}{3}L=2$, to its value on S^3 , R , or

$$L = \frac{2}{3}R; \quad (167)$$

and we use that on T^3 instantons are relevant for $z = m_{0^+} L > 5$ [32, 33]. Furthermore, we assume that the scalar glueball masses are roughly equal in both geometries at these volumes. These low values of $m_{0^+} R$ are not reached in the tree level approach, but we do reach them in the one-loop case which shows that it was necessary to include the one-loop corrections. This regime of masses occurs for values of the coupling where we expect our model to still be valid. Specifically, $m_{0^+} R = 1.4$ corresponds to $f = 0.28$. At larger couplings, we clearly see that the wave functional feels too much of the boundary of the fundamental domain. For $f = 0.4$ this is dramatically clear from fig. 11, where the wave function is seen to probe unacceptable regions of the boundary of the fundamental domain to remain a good approximation to the full wave function. From fig. 8 we see that the scalar and tensor masses even cross around $f = 0.33$, which is certainly unacceptable for the full theory. Clearly we have pushed the model passed its region of validity for $f > 0.3$.

Of course, at some point $m_{0^+} R$ has to start to rise again, and when m_{0^+} reaches its asymptotic in finite-volume value, $m_{0^+} R$ grows linearly with R . Both the truncated and the one-loop results show that $m_{0^+} R$ exhibits a minimum, after which it starts to rise again. It rises linearly in f for $f \rightarrow 1$, as follows from the strong coupling results in fig. 5, which are also valid for the one-loop case. This however does not mean that we are approaching the infinite-volume limit, because our effective model is certainly not fit to describe this regime. Moreover, it is clear that no statements can be made on the R dependence of f for these large couplings and volumes.

Other indications that our results are in the domain of expected validity are that at $f = 0.25$ the tensor to scalar mass ratio is given by 1.5, rising from 1 at zero coupling to 1.8 at $f = 0.28$, see g. 9. For a torus geometry one finds a similar range. Below $z = m_{0^+} L = 5$ the tensor is split into a doublet at $0.9m_{0^+}$ and a triplet at $1.7m_{0^+}$ [32, 34] (due to breaking of rotational to cubic invariance), whereas these states seem to merge at $z > 7$ into a degenerate quintet with $m_{2^+} = 1.5m_{0^+}$.

We assume that in intermediate volumes the two-loop β function can be used to convert the dependence on the relevant coupling constants to the dependence on the radius R or the size L . Thus, for R we have ($f = g^2/(2^2)$)

$$(\beta_R R)^2 = \beta_1 g^2 \frac{-2}{1} e^{\frac{1}{19g^2}}; \quad \beta_1 = \frac{11}{24^2}; \quad \frac{-2}{1} = \frac{102}{121}; \quad (168)$$

and the same formula holds for L in terms of the minimal subtraction coupling g_{MS} . If we, as usual, set the scale by a string tension of $\sigma = (425 \text{ MeV})^2$ and use that $\beta_{\overline{MS}} = m_{0^+} = 0.3$ for T^3 , we have that in physical units $z = m_{0^+} L = 5$ corresponds to $L = 0.7 \text{ fm}$ and hence, using eq. (167), to $R = 0.19 \text{ fm}$. As derived earlier, this corresponds to $f = 0.28$ on the three-sphere, and eq. (168) gives $\beta_R = 1.3 \text{ fm}^{-1}$. On the torus, $z = 5$ corresponds to $g_{MS} = 2.42$ [2]. Relating this to $L = 0.7 \text{ fm}$ gives $\beta_L = 0.39 \text{ fm}^{-1}$. In this way we can compare our result for $m_{2^+} = m_{0^+}$ as a function of the volume to the doublet E^+ and the triplet T_2^+ on the torus, as is shown in g. 12. The vertical bar on the right indicates the range of lattice Monte Carlo values [34] for the E^+ and T_2^+ masses (equal within errors) at $L = 1$ to 1.5 fm .

Another way to relate the length scales above to a value of the coupling constant uses the definition of the running coupling constant in [35] and the relation between this coupling constant and the one in the \overline{MS} scheme. Proceeding in this way relates $R = 0.19 \text{ fm}$ to a value for f of 0.26, which is yet another indication that this regime for the coupling constant corresponds to volumes where the instanton effects are important. To obtain this number we correct for the finite renormalizations appearing in eq. (119) and we assumed that setting the linear size L of the d -dimensional torus to R gives the \overline{MS} scheme. This ambiguity could be fixed by computing the effective hamiltonian using e.g. Pauli-Villars regularization and the known relation to the minimal subtraction scheme. In our calculations f is however just a parameter that allows us to probe different volumes and its precise relation to the physical scale is not so relevant.

Returning to g. 12, we can distinguish three regimes in R . For small R , we expect the finite-size effects, like the effect of the curvature of S^3 , to be large. The masses in the effective model, although perturbatively calculable, will therefore not correspond to the masses on the torus. In this regime the smallest mass in the 000-odd sector 0 (see g. 9) is actually smaller than the mass of the scalar glueball 0^+ , an effect that also can be seen from the perturbative evaluation of the energy levels eq. (163) and (164). This we expect to be a consequence of the strong finite size effects that are visible at small values of R .

Around $R = 0.1 \text{ fm}$, corresponding to $L = 0.36 \text{ fm}$, we see (in the sphere geometry) the masses deviate from the perturbative expansion, signalling the onset of the instantons. They drive the tensor to scalar ratio in the right direction, that is, towards the large-volume value of 1.5. The mass of the odd glueball is now higher than that of the even glueball. Apparently the non-perturbative effects also drove this quantity towards more physical

values: from lattice calculations a value of $m(0) = m(0^+) \approx 1.7$ can be extracted [36], compatible with what is found here.

For $R > 0.2 \text{ fm}$, our effective model is no longer valid, due to the spreading out of the wave functional over the boundary of the fundamental domain, as discussed before.

Finally, an important goal of this project was to get results for glueball masses as a function of β . The truncated results showed a pronounced dependence on β in the regime where boundary effects are appreciable (see fig. 6). Quite remarkably, and unexpectedly, this strong dependence disappears when adding the one-loop corrections. In particular, at $\beta = 0$ and $\beta = \beta_c$, where boundary conditions can be implemented most accurately, the masses do not differ significantly (see fig. 10). Caution needs to be applied in concluding that the same will hold at large volumes, but in any case it would be interesting if glueball masses could be measured at $\beta = \beta_c$ on the lattice as comparison.

In conclusion, we should expect our one-loop corrected result to be a relatively accurate representation of the true masses on S^3 up to $\beta = 0.28$ corresponding to a circumference of approximately 1.3 fm , up to where also the variational basis does not exhibit too much of the problems with the Temple bound (cf. fig. 8). The approach to infinite-volume values of results on the three-sphere, as compared to torus results, is slow. We typically have a dependence on powers of $1/R$ as compared to an exponential behaviour in L [16]. As our results should not be expected to be already in the asymptotic domain, the rough agreement we find with results on the torus is gratifying.

When comparing the truncated and one-loop corrected results, the results for the dependence show that strong non-linear and non-perturbative effects influence the spectrum. We have shown there is a small, but finite window from $R = 0.1 \text{ fm}$ to $R = 0.2 \text{ fm}$ (at smaller volumes everything can be described perturbatively) where these effects can be included reliably, showing convincingly how important the global properties of the field space are for the non-perturbative dynamics of non-abelian gauge theories.

Acknowledgments

The author wishes to thank Pierre van Baal for many helpful discussions. He also wishes to thank D. Schutte for useful discussions. Support by Stichting Nationale Computer Faciliteiten (NCF) for use of the Cray Y-MP at SARA was appreciated.

Appendices

A Details on the basis

In this appendix we will exploit the relation between S^3 and $SU(2)$ to rederive the basis (12). After this we will make the link with the definition of functions on S^n in terms of homogeneous polynomials in the coordinates of the embedding space.

A.1 The SU(2) group structure of S^3

There is a one-to-one correspondence between points of S^3 and SU(2) given by $g = n$. For instance, the matrix V_j^i of eq. (6) can in this light be seen as the adjoint representation of SU(2). The group of spatial symmetries of S^3 is SO(4). These symmetries correspond to the left and right symmetries on SU(2). Let ψ be a function on SU(2) or equivalently on S^3 . SU(2) can now act on this function by left or right multiplication:

$$D^L(g_1)\psi(g) = \psi(g_1^{-1}g); \quad D^R(g_2)\psi(g) = \psi(gg_2); \quad g, g_1, g_2 \in \text{SU}(2); \quad (169)$$

These infinite-dimensional representations of the group SU(2) induce representations of the Lie algebra $\mathfrak{su}(2)$. We will show that the generators L of these representations correspond to L_1 and L_2 :

$$\begin{aligned} iL_j^L \psi(g) &= \frac{d}{dt} (\exp(it\frac{1}{2}\tau_j)g) \Big|_{t=0} \\ &= \frac{d}{dt} (n + \frac{1}{2}t\tau_j n) \Big|_{t=0} \\ &= \frac{d}{dt} (n + \frac{1}{2}t\tau_j n) \Big|_{t=0} \\ &= \frac{1}{2} \tau_j n \frac{\partial}{\partial x} (n) = iL_1^j (n); \end{aligned} \quad (170)$$

According to the Peter-Weyl theorem [37], a basis of functions on SU(2) is provided by the collection of matrix elements of all the finite-dimensional unitary irreducible representations of SU(2). The relation of these matrix elements with the basis of eq. (12) is

$$h_{jlm_L m_R} = (-1)^{m_L} \sqrt{\frac{2l+1}{2l+1}} D_{m_L m_R}^l(g); \quad (171)$$

A.2 The eigenfunctions of the laplacian on S^n

In this section we summarize some well-known facts about the spectrum of the laplacian on an n -dimensional sphere. This allows us to identify the functions (12) with explicit functions on S^3 . Let x_0, \dots, x_n be coordinates in \mathbb{R}^{n+1} . Using radial coordinates $r, \theta_1, \dots, \theta_n$ one can explicitly solve for the eigenfunctions of the spherical laplacian Δ_n , using separation of variables and recursion in n . The result of this calculation (cf. e.g. [37]) is that the spectrum is given by

$$f_{L, (L+n-1)} g_{L=0;1;2;\dots;}; \quad (172)$$

and the degeneracy of the level L is given by

$$\frac{(L+n)!}{n!} \frac{(L-1)!}{(L-2+n)!}; \quad (173)$$

We will relate these eigenfunctions to polynomials in x . Let V^L be the set of polynomials in x that are homogeneous of degree L . To such a polynomial p corresponds a function Y on S^n defined by

$$p(x_0, \dots, x_n) = r^L Y(\theta_0, \dots, \theta_n); \quad (174)$$

Suppose that p is a harmonic polynomial, i.e. $\Delta p = 0$. We then have

$$0 = \frac{1}{r^n} \frac{\partial}{\partial r} r^n \frac{\partial}{\partial r} + \frac{1}{r^2} \Delta_{S^n} r^L Y = L(L+n-1) r^{L-2} Y + r^{L-2} \Delta_{S^n} Y : \quad (175)$$

We have found that every harmonic polynomial of degree L corresponds to a function on the n -sphere that is an eigenfunction of the spherical Laplacian with eigenvalue $-L(L+n-1)$. The number of monomials of degree L in the variables x_0, \dots, x_n is given by

$$\dim(V^L) = \binom{L+n}{n} : \quad (176)$$

Hence we have

$$\begin{aligned} \dim(\text{Ker}(\Delta)) &= \dim(V^L) - \dim(\text{Im}(\Delta)) \\ &= \binom{L+n}{n} - \binom{L-2+n}{n} \\ &= \binom{L+n}{n} - \binom{L-2+n}{n} : \end{aligned} \quad (177)$$

Since we know the degeneracy of the eigenvalue $-L(L+n-1)$, we have shown that all the eigenfunctions of the spherical Laplacian correspond to harmonic polynomials. Moreover, the inequality in the last equation is actually an equality.

For the case of S^2 the eigenfunctions are the well-known spherical harmonics Y_M^L . For the case S^3 the spectrum becomes $-L(L+2)g_{L=0,1,2,\dots}$, with the degeneracy given by

$$\binom{L+3}{3} - \binom{L+1}{3} = (L+1)^2 : \quad (178)$$

When comparing this with the results (171), we see that $L = 2l$. The four $l = \frac{1}{2}$ modes $\{x_j\}_{j=1}^4$ are linear combinations of the four scalar functions x_j ; ($j = 0, \dots, 3$), whereas the nine $l = 1$ modes $\{x_j\}_{j=1}^9$ correspond to the nine components of V_j^1 .

In section 4 the results of this appendix are applied to S^8 .

B The linear term in the path integral

In this appendix we show that the term $J \cdot Q$ in eq. (116) does not make a contribution to the effective action up to the order we are interested in: the lowest order contribution from J to the effective potential will be of the form $c^4 d^2$ and $c^2 d^4$.

The crucial remark is that in the path integral the constant modes are excluded from the integration over Q_0 , and the $(c;d)$ modes are excluded from the integration over Q_i . This means that one must remember to put projectors $(1-P)$ around operators like W , and replace source currents like J with $((1-P)J)$. We will show that after this projection J contains only terms that are cubic in B .

We have $F_{0i} = F_{i0} = B_i$ and $F_{ij} = 2\epsilon_{ijk}(c_k - d_k) + [B_i, B_j]$, with $B_i = c_i + d_i$. This implies $J_0 = D \cdot F_0 = [B_i, B_i]$ and $J_j = D \cdot F_j = B_j + D_i F_{ij}$. In our approximation

we are only interested in the term $D_i F_{ij} = J_j^{(1)} + J_j^{(2)} + J_j^{(3)}$, where $J^{(n)}$ is of order n in the field B . From $D_i F_{ij} = \partial_i F_{ij} - \epsilon_{ijk} F_{ik} + [A_i; F_{ij}]$, we obtain

$$J_j^{(1)} = 4c_j; \quad (179)$$

$$J_j^{(2)} = 3\epsilon_{ijk} [c_i; c_k] - 3\epsilon_{mnp} [d_m; d_n] N_j^p; \quad (180)$$

$$\begin{aligned} J_j^{(3)} &= [B_i; [B_i; B_j]] \\ &= [c_i; [c_i; c_j]] + [d_i; [d_i; c_j]] \\ &\quad + [c_i; [c_i; d_j]] + [d_i; [d_i; d_j]] \\ &\quad + [d_i; [c_i; c_j]] + [c_i; [d_i; c_j]] \\ &\quad + [d_i; [c_i; d_j]] + [c_i; [d_i; d_j]] \end{aligned} \quad (181)$$

This directly implies that $(1 - P_V)J^{(1)} = (1 - P_V)J^{(2)} = 0$. The first four terms of $J^{(3)}$ do not contribute since they too are modes with $(l; k) = (0; 1)$ or $(l; k) = (1; 0)$. We write the last four terms of $J^{(3)}$ as follows:

$$A_{ij}^p V_i^p + B_i^{mn} V_i^m V_j^n; \quad (182)$$

with the $su(2)$ -valued constants

$$A_{ij}^p = [d_p; [c_i; c_j]] + [c_i; [d_p; c_j]]; \quad B_i^{nm} = [d_m; [c_i; d_n]] + [c_i; [d_m; d_n]]; \quad (183)$$

The matrices A^p and B_i can be decomposed in a trace part, an antisymmetric part and a symmetric traceless part. For the A^p terms, this is the decomposition into $(l; k)$ is $(1; 0)$, $(1; 1)$ and $(1; 2)$ respectively. For the B_i terms, it gives the split in the three possible l values $(0; 1)$, $(1; 1)$ and $(2; 1)$. Projecting out the $(c; d)$ modes from J_i , we obtain

$$(1 - P_V)J_j = A_{ij}^p V_i^p + B_i^{mn} V_i^m V_j^n; \quad (184)$$

where A and B are obtained from the A and B of eq. (183) by projecting out the trace part.

Expanding the path integral of eq. (116) gives diagrams with interactions of the Q field with the source $J(B)$. If we also take along the Q^3 , BQ^3 and Q^4 terms in the action, diagrams with only one occurrence of J can in principle give a contribution of the order $c^2 d^2$. However, in order to obtain a $c^2 d^2$ invariant, we must take the trace part of A and B . Since these trace parts are zero, we see that a single occurrence of J can not give rise to contributions of the order $c^2 d^2$.

C Angular matrix elements

We will perform the reduction of the matrix elements of the operator A of eq. (145) to reduced matrix elements. We use eq. (132).

$$\begin{aligned} & h_j^{0; m^0; i_1^0; i_2^0} A_{jj; m; i_1; i_2} \\ &= h_n^{0; m^0; l_1^0; l_2^0; 1^0; 1^0; 2^0; 2^0} \circ \\ & \quad j; 0; l_1; l_2; 0; 1; l_2; 0; 2 i_{jj; m; l_1; l_2; 1; 1; l_2; l_2; 2 i} \end{aligned}$$

$$\begin{aligned}
&= \sum_{m_1^0, m_2^0} X \binom{0}{1}^{l_1^0 \quad l_2^0 + m_1^0} \frac{1}{2j^0 + 1} \begin{matrix} l_1^0 & l_2^0 & j^0 \\ m_1^0 & m_2^0 & m^0 \end{matrix} A \\
&\quad \sum_{m_1, m_2} X \binom{0}{1}^{l_1 \quad l_2 + m} \frac{1}{2j + 1} \begin{matrix} l_1 & l_2 & j \\ m_1 & m_2 & m \end{matrix} A \\
&\quad \sum_{m_s^0, m_s} X \binom{0}{1}^{l_s^0 \quad m_s^0} \frac{1}{2l_s^0 + 1} \binom{0}{1}^{l_s \quad m_s} \frac{1}{2l_s + 1} \binom{0}{1}^{l_s \quad m_s} \frac{1}{2l_s + 1} \\
&\quad hL_{1s}^{0; l_s^0; l_1^0; \quad 0; m_s^0; m_1^0} f \tilde{f}_{1s; l_s; 0; \sim; m_s; 0} i \tilde{l}_{1s; l_s; l_1; \quad 1; m_s; m_1} ig \\
&\quad hL_{2s}^{0; l_s^0; l_2^0; \quad 0; m_s^0; m_2^0} f \tilde{f}_{2s; l_s; 0; \sim; m_s; 0} i \tilde{l}_{2s; l_s; l_2; \quad 2; m_s; m_2} ig: \quad (185)
\end{aligned}$$

We introduce reduced matrix elements through

$$\begin{aligned}
&hL_{1s}^{0; l_s^0; l_1^0; \quad 0; m_s^0; m_1^0} f \tilde{f}_{1s; l_s; 0; \sim; m_s; 0} i \tilde{l}_{1s; l_s; l_1; \quad 1; m_s; m_1} ig = \\
&\quad \binom{0}{1}^{m_s^0 + m_1^0} \begin{matrix} l_s^0 & l_s & l_s \\ m_s^0 & m_s & m_s \end{matrix} A \begin{matrix} l_1^0 & 0 & l_1 \\ m_1^0 & 0 & m_1 \end{matrix} A F(l_1^0; l_1; i_1): \quad (186)
\end{aligned}$$

Using

$$\begin{matrix} 0 \\ \oplus \end{matrix} \begin{matrix} l_1^0 & 0 & l_1 \\ m_1^0 & 0 & m_1 \end{matrix} A = \binom{0}{1}^{l_1 \quad m_1} \frac{1}{2l_1 + 1} \begin{matrix} l_1^0 & 0 & l_1 \\ m_1^0 & 0 & m_1 \end{matrix} A; \quad (187)$$

the summations over m_1^0 and m_2^0 become trivial. The remaining summations in eq. (185) can then be dealt with using twice the completeness relation

$$\sum_{m_1, m_2} \begin{matrix} 0 \\ \oplus \end{matrix} \begin{matrix} j_1 & j_2 & j_3 \\ m_1 & m_2 & m_3 \end{matrix} A \begin{matrix} 1 \quad 0 \\ \oplus \end{matrix} \begin{matrix} j_1 & j_2 & j_3 \\ m_1 & m_2 & m_3^0 \end{matrix} A = \frac{1}{2j_3 + 1} \begin{matrix} j_3^0 & j_3 & m_3^0 \\ m_3^0 & m_3 & m_3 \end{matrix} (j; j; j); \quad (188)$$

where $(j; j; j) = 1$ if j_1, j_2 and j_3 satisfy the triangular condition, and is zero otherwise. We obtain

$$\begin{aligned}
&h j^0; m^0; i_1^0; i_2^0 A j j; m; i_1; i_2 i = \\
&\quad \begin{matrix} l_1^0 & l_2^0 & j^0 \\ m_1^0 & m_2^0 & m^0 \end{matrix} \begin{matrix} l_1 & l_2 & j \\ m_1 & m_2 & m \end{matrix} \begin{matrix} l_s^0 & l_s & l_s \\ m_s^0 & m_s & m_s \end{matrix} \frac{F(i_1^0; l_1; i_1) F(i_2^0; l_2; i_2)}{(2l_s^0 + 1)(2l_s + 1)(2l_s + 1)^{\frac{1}{2}}}: \quad (189)
\end{aligned}$$

We absorbed the factors $\binom{0}{1}^{l_i} (2l_i + 1)^{-1/2}$ for $i = 1, 2$ in the F functions. We can evaluate the F functions by setting in eq. (186)

$$m_1^0 = m_1 = l_1; \quad m_s = l_s; \quad m_s^0 = l_s^0; \quad m_s = l_s^0 \quad l_s: \quad (190)$$

Thus we find

$$\begin{aligned}
&F(i^0; l; i) = \binom{0}{1}^{l_s^0} \begin{matrix} l_s^0 & l_s & l_s \\ m_s^0 & m_s & m_s \end{matrix} A \\
&\quad hL_{1s}^{0; l_s^0; l_1^0; \quad 0; m_s^0; m_1^0} f \tilde{f}_{1s; l_s; 0; \sim; m_s; 0} i \tilde{l}_{1s; l_s; l_1; \quad 1; m_s; m_1} ig: \quad (191)
\end{aligned}$$

Note that the only dependence of the matrix elements on j is through the triangular condition on l_1, l_2 and j . Also note that the explicit functions

$$l_1^0 l_1 \quad l_2^0 l_2 \quad \left(\begin{smallmatrix} 0 \\ s \end{smallmatrix}; \begin{smallmatrix} 0 \\ s \end{smallmatrix}; \begin{smallmatrix} 0 \\ s \end{smallmatrix} \right) \quad (192)$$

are superfluous: they are also contained within the F functions. The $(l_1; l_2; j)$ function can be deleted too: the corresponding triangular condition is satisfied from the beginning.

Specializing to the case where A only depends on c , we have $\gamma_s = 0$ and we can also absorb the factors $(-1)^{l_s} (2l_s + 1)^{-1/2}$ in F . We have for instance

$$h_j^{0; m^0; i_1^0; i_2^0} j \text{inv}_3(\hat{c}) jj; m; i_1; i_2 i = j^{0j} m^{0m} F_3(i_1^0; i_1) \left(\begin{smallmatrix} 0 \\ 2 \end{smallmatrix}; i_2 \right); \quad (193)$$

with

$$F_3(i^0; i) = h_L^{0; l_s^0; l_r^0; 0; l_s^0; l_r^0} j \text{inv}_3(\hat{c}) j; l_s; l_r; i; l_s; l_r i; \quad (194)$$

We similarly treat $\text{inv}_4(\hat{c})$, $\text{inv}_6(\hat{c})$, $\text{inv}_7(\hat{c})$ and $\text{inv}_8(\hat{c})$ which give rise to the reduced matrix elements F_4, F_6, F_7 and F_8 respectively. Operators that depend only on d and operators that are products of a function of c and of a function of d pose no problems either. We have for instance

$$h_j^{0; m^0; i_1^0; i_2^0} j \text{inv}_3(\hat{d}) jj; m; i_1; i_2 i = j^{0j} m^{0m} \left(\begin{smallmatrix} 0 \\ 1 \end{smallmatrix}; i_1 \right) F_3(i_2^0; i_2); \quad (195)$$

$$h_j^{0; m^0; i_1^0; i_2^0} j \text{inv}_3(\hat{c}) \text{inv}_3(\hat{d}) jj; m; i_1; i_2 i = j^{0j} m^{0m} F_3(i_1^0; i_1) F_3(i_2^0; i_2); \quad (196)$$

The operator $\text{inv}_2(c; d)$ is treated with the general formulae eq. (189) and (191). One can show $\text{inv}_2(\hat{c}; \hat{d}) = \frac{1}{9} \frac{1}{99} 5 h_{\hat{c} \hat{d}}^{0; 0; 0; 0; 2; 2; 0; 1; 2; 0; 1} i$. Using eq. (191) we define

$$F_{22}(i^0; i) = (-1)^{l_s^0} \begin{smallmatrix} 0 & & 1 & 1 \\ & l_s^0 & 2 & l_s^0 \\ & l_s^0 & l_s^0 & l_s^0 \end{smallmatrix} A \quad h_L^{0; l_s^0; l_r^0; 0; l_s^0; l_r^0} j f f; 2; 2; 0; 1; l_s^0 \quad l_s; 0 i j; l_s; l_r; i; l_s; l_r i g; \quad (197)$$

and we obtain

$$h_j^{0; m^0; i_1^0; i_2^0} j \text{inv}_2(\hat{c}; \hat{d}) jj; m; i_1; i_2 i = j^{0j} m^{0m} \begin{smallmatrix} < \\ 9 \end{smallmatrix} \left(\begin{smallmatrix} 0 \\ 1 \end{smallmatrix}; i_1 \right) \left(\begin{smallmatrix} 0 \\ 2 \end{smallmatrix}; i_2 \right) \frac{1}{99} \frac{F_{22}(i_1^0; i_1) F_{22}(i_2^0; i_2)}{[(2l_s^0 + 1)(2l_s + 1)]^{\frac{1}{2}}}; \quad (198)$$

For products like $\text{inv}_3(c) \text{inv}_2(c; d)$ we obtain

$$h_j^{0; m^0; i_1^0; i_2^0} j \text{inv}_3(\hat{c}) \text{inv}_2(\hat{c}; \hat{d}) jj; m; i_1; i_2 i = j^{0j} m^{0m} \begin{smallmatrix} < \\ 9 \end{smallmatrix} F_3(i_1^0; i_1) \left(\begin{smallmatrix} 0 \\ 2 \end{smallmatrix}; i_2 \right) \frac{1}{99} \frac{F_{52}(i_1^0; i_1) F_{22}(i_2^0; i_2)}{[(2l_s^0 + 1)(2l_s + 1)]^{\frac{1}{2}}}; \quad (199)$$

with

$$F_{52}(i^0; i) = (-1)^{l_s^0} \begin{smallmatrix} 0 & & 1 & 1 \\ & l_s^0 & 2 & l_s^0 \\ & l_s^0 & l_s^0 & l_s^0 \end{smallmatrix} A \quad h_L^{0; l_s^0; l_r^0; 0; l_s^0; l_r^0} j f \text{inv}_3(\hat{c}) j; 2; 2; 0; 1; l_s^0 \quad l_s; 0 i j; l_s; l_r; i; l_s; l_r i g; \quad (200)$$

Similarly the operator $\text{inv}_4(c) \text{inv}_2(c;d)$ leads to the reduced matrix element F_{62} .

The only operator in V^2 that we have yet to deal with is $\text{inv}_2^2(c;d)$. For this operator we need to construct the spectral decomposition. We write

$$\begin{aligned} \text{inv}_2^2 = & a \mathfrak{D};0;4;4;0;1;4;0;1i + b \mathfrak{D};0;2;4;0;1;4;0;1i \\ & + c \mathfrak{D};0;0;4;0;1;4;0;1i + d \mathfrak{D};0;2;2;0;1;2;0;1i \\ & + e (\mathfrak{D};0;2;4;0;1;2;0;1i + \mathfrak{D};0;2;2;0;1;4;0;1i) \\ & + f (\mathfrak{D};0;0;4;0;1;0;0;1i + \mathfrak{D};0;0;0;0;1;4;0;1i) \\ & + g \mathfrak{D};0;0;0;0;1;0;0;1i: \end{aligned} \quad (201)$$

Using the explicit formulae for the corresponding polynomials, we solve for the coefficients $a;:::g$. The new reduced matrix elements we need are F_{44} , F_{42} and F_{40} for the operators with $(\mathbb{L};\mathbb{L}_s;\mathbb{L}_r)$ respectively $(4;4;0)$, $(4;2;0)$ and $(4;0;0)$. The function F_{40} can be obtained from F_4 using the relation

$$\text{inv}_4(\mathbb{C}) = \frac{1}{22} + \frac{1}{22} \frac{r}{39} h\mathbb{C};4;0;0;1;0;0i: \quad (202)$$

The result is

$$h\mathfrak{j}^0;m^0;i_1^0;i_2^0 \text{inv}_2^2(\mathbb{C};\hat{d}) \mathfrak{j}\mathfrak{j};m;i_1;i_2i = \mathfrak{j}^0\mathfrak{j} \mathfrak{m}^0\mathfrak{m} : \frac{A}{[(2\mathbb{L}_s^0 + 1)(2\mathbb{L}_s + 1)]^{\frac{1}{2}}} + B \frac{9}{\mathbb{L}_s}; \quad (203)$$

with

$$\begin{aligned} A = & \frac{2}{11583} F_{44}(i_1^0;i_1) F_{44}(i_2^0;i_2) \\ & + \frac{4}{50193} F_{42}(i_1^0;i_1) F_{42}(i_2^0;i_2) - \frac{4}{1859} F_{22}(i_1^0;i_1) F_{22}(i_2^0;i_2) \\ & - \frac{1}{1859} \frac{56}{2187} (F_{42}(i_1^0;i_1) F_{22}(i_2^0;i_2) + F_{22}(i_1^0;i_1) F_{42}(i_2^0;i_2)); \end{aligned} \quad (204)$$

$$\begin{aligned} B = & \frac{16}{45} F_4(i_1^0;i_1) F_4(i_2^0;i_2) - \frac{4}{135} (F_4(i_1^0;i_1) \left(\frac{0}{2};i_2\right) + \left(\frac{0}{1};i_1\right) F_4(i_2^0;i_2)) \\ & + \frac{2}{135} \left(\frac{0}{1};i_1\right) \left(\frac{0}{2};i_2\right); \end{aligned} \quad (205)$$

References

- [1] M. Luscher, Nucl. Phys. B219 (1983) 233.
- [2] J. Koller and P. van Baal, Nucl. Phys. B302 (1988) 1; P. van Baal, Acta Phys. Pol. B20 (1989) 295.
- [3] H. D. Politzer, Phys. Rev. Lett. 30 (1973) 1346; D. J. Gross and F. Wilczek, Phys. Rev. Lett. 30 (1973) 1343; S. Coleman and D. J. Gross, Phys. Rev. Lett. 31 (1973) 851.
- [4] N. M. Christ and T. D. Lee, Phys. Rev. D22 (1980) 939.
- [5] I. Singer, Comm. Math. Phys. 60 (1978) 7.
- [6] O. Babelon and C. Viallet, Comm. Math. Phys. 81 (1981) 515.

- [7] V . G r i b o v , Nucl. Phys. B139 (1978) 1.
- [8] A . Belavin , A . Polyakov , A . Schwarz and Y . Tyupkin , Phys. Lett. B59 (1975) 85;
M . Atiyah , V . D r i n f e l d , N . H i t c h i n and Yu . M a n i n , Phys. Lett. A 65 (1978) 185.
- [9] F R . K l i n k h a m e r and N . M a n t o n , Phys. Rev. D 30 (1984) 2212.
- [10] M A . S e m e n o v - T y a n - S h a n s k i i and V A . F r a n k e , Zapiski Nauchnykh Sem inarov
Leningradskogo O t d e l e n i y a M a t e m a t i c h e s k o g o I n s t i t u t a i m . V A . S t e k l o v A N S S S R ,
120 (1982) 159. Translation: (P l e n u m P r e s s , New York , 1986) p . 1999.
- [11] D . Z w a n z i g e r , Nucl. Phys. B412 (1994) 657.
- [12] P . v a n B a a l and B M . v a n d e n H e u v e l , Nucl. Phys. B417 (1994) 215.
- [13] A S . K r o n f e l d and P . v a n B a a l , Nucl. Phys. B (P r o c . S u p p l .) 9 , (1989) 227.
- [14] M . G a r c a P e r e z e t a l , Nucl. Phys. B413 (1994) 535.
- [15] P . v a n B a a l and N D . H a r i D a s s , Nucl. Phys. B385 (1992) 185.
- [16] M . L u s c h e r , C o m m . M a t h . P h y s . 104 (1986) 177.
- [17] R E . C u t k o s k y , J . M a t h . P h y s . 25 (1984) 939; R E . C u t k o s k y and K . W a n g , Phys.
Rev. D37 (1988) 3024; R E . C u t k o s k y , C z e c h . J . P h y s . 40 (1990) 252.
- [18] B M . v a n d e n H e u v e l , hep-lat/9604017, to appear in Physics Letters B .
- [19] B M . v a n d e n H e u v e l , Phys. Lett. B368 (1996) 124.
- [20] G . ' t H o o f t , Phys. Rev. D14 (1976) 3432.
- [21] R . J a c k i w , in Current algebra and anomalies, (W o r l d S c i e n t i c , Singapore , 1985) p .
211.
- [22] P . v a n B a a l , Nucl. Phys. B351 (1991) 183.
- [23] M . L u s c h e r , A n n . P h y s . 142 (1982) 359.
- [24] J A M . V e r m a s e r e n , S y m b o l i c m a n i p u l a t i o n w i t h F O R M , (C o m p u t e r A l g e b r a N e d e r -
l a n d , A m s t e r d a m , 1991).
- [25] C . B l o c h , Nucl. Phys. 6 (1958) 329.
- [26] S . W o l f r a m e t a l , M a t h e m a t i c a , (A d d i s o n - W e s l e y , New York , 1991).
- [27] A R . E d m o n d s , A n g u l a r m o m e n t u m i n q u a n t u m m e c h a n i c s , (P r i n c e t o n U n i v e r s i t y
P r e s s , P r i n c e t o n , 1957).
- [28] B M . v a n d e n H e u v e l , N o n - p e r t u r b a t i v e p h e n o m e n a i n g a u g e t h e o r y o n S^3 , (P h . D .
t h e s i s , L e i d e n , S e p t e m b e r 1996).

- [29] M . Reed and B . Simon, Methods of modern mathematical physics, vol. 4 (Academic Press, New York, 1978).
- [30] T . Kato, J. Phys. Soc. Japan 4 (1949) 334.
- [31] M . Abramowitz and I A . Stegun, Handbook of mathematical functions, (Dover publications, New York).
- [32] P . van Baal, Acta Phys. Pol. B20 (1989) 295.
- [33] J . Hoek, Phys. Lett. B219 (1989) 92.
- [34] B . Carpenter, C . Michael and M . J. Teper, Phys. Lett. B198 (1987) 511; C . Michael, G A . Tickle and M . J. Teper, Phys. Lett. B207 (1988) 313.
- [35] M . Luscher, R . Narayanan, P . Weisz, U . Wol, Nucl. Phys. B384 (1992) 168; M . Luscher, R . Sommer, U . Wol and P . Weisz, Nucl. Phys. B389 (1993) 247.
- [36] C . Michael and M . Teper, Phys. Lett. B199 (1987) 95.
- [37] A O . Barut and R . Raczyka, Theory of group representations and applications, (Polish Scientific Publishers, Warsaw, 1977).

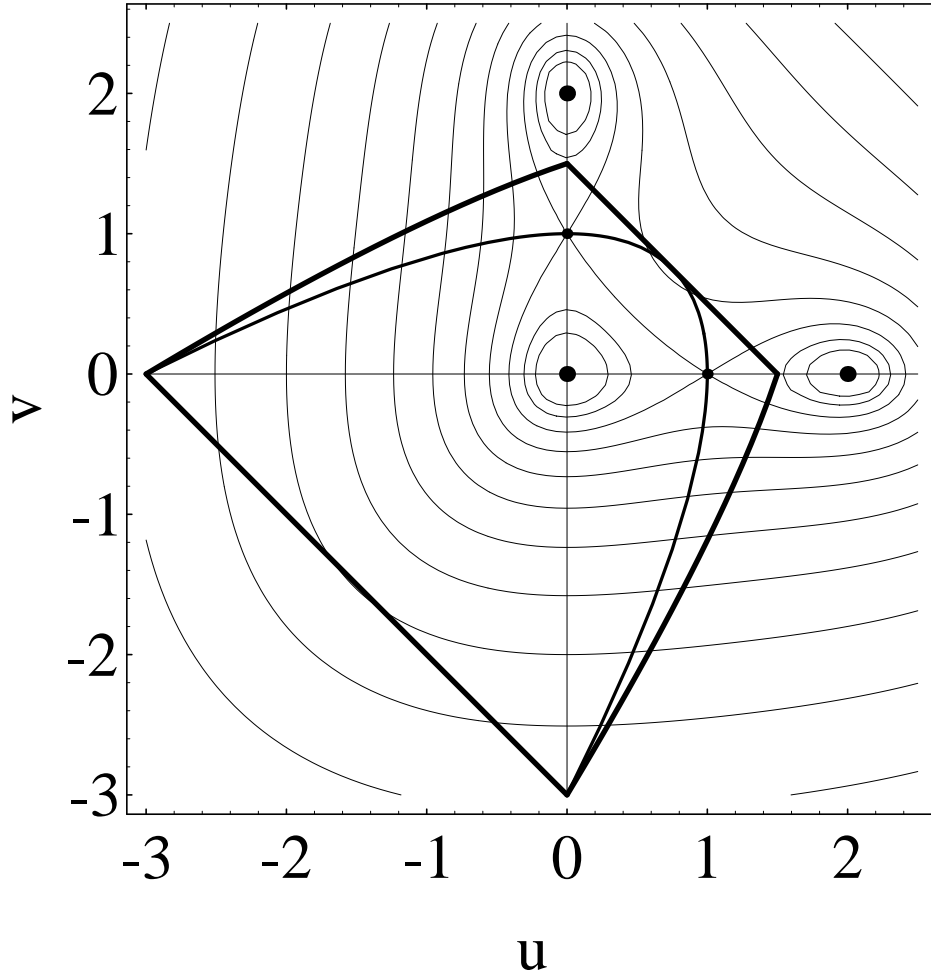


Figure 1: The $(u;v)$ plane: a two-dimensional subspace of \mathcal{A} . Location of the classical vacua, sphalerons, lines of equal potential. The boundary of the fundamental domain lies between the Gibbons horizon (fat sections) and the lower bound \tilde{v} (drawn parabola): $\tilde{v} = -u^2/4$, with the Gibbons region.

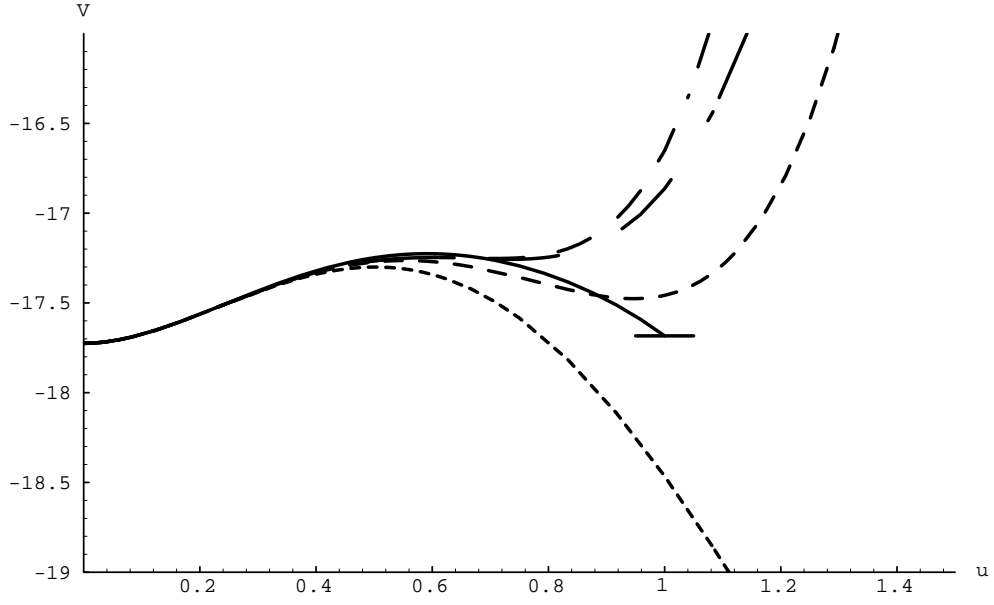


Figure 2: Expansion of $V^{(1)}(u)$ in the tunnelling parameter u . We dropped the \hbar and $\log(L)$ dependent parts. We have drawn the expansion up to order u^4 , u^6 , u^8 and u^{10} . Longer dashes correspond to higher order expansions. The horizontal line at $u = 1$ denotes the exact potential at the sphaleron, the drawn curve is the sixth order t explained in the text.

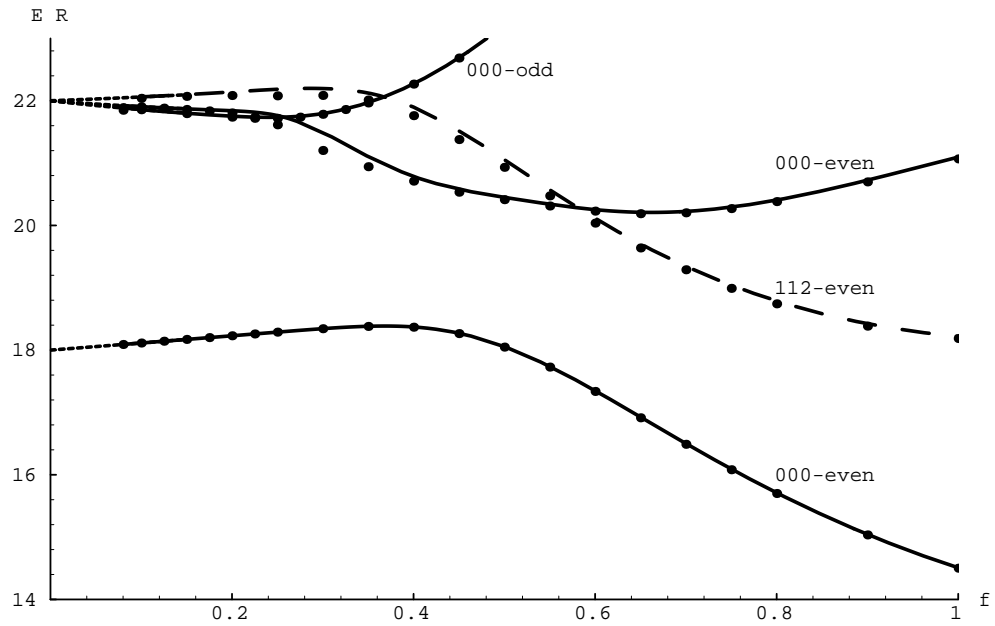


Figure 3: Lowest energy levels for $\alpha = 0$. Drawn curves correspond to levels in the $(0;0;0)$ sector. The dashed curve denotes the ground level in the $(1;1;2)$ -even sector. The short-dashed curves are the perturbative expansions, and the individual dots are lower bounds on the levels as obtained by Temple's inequality.

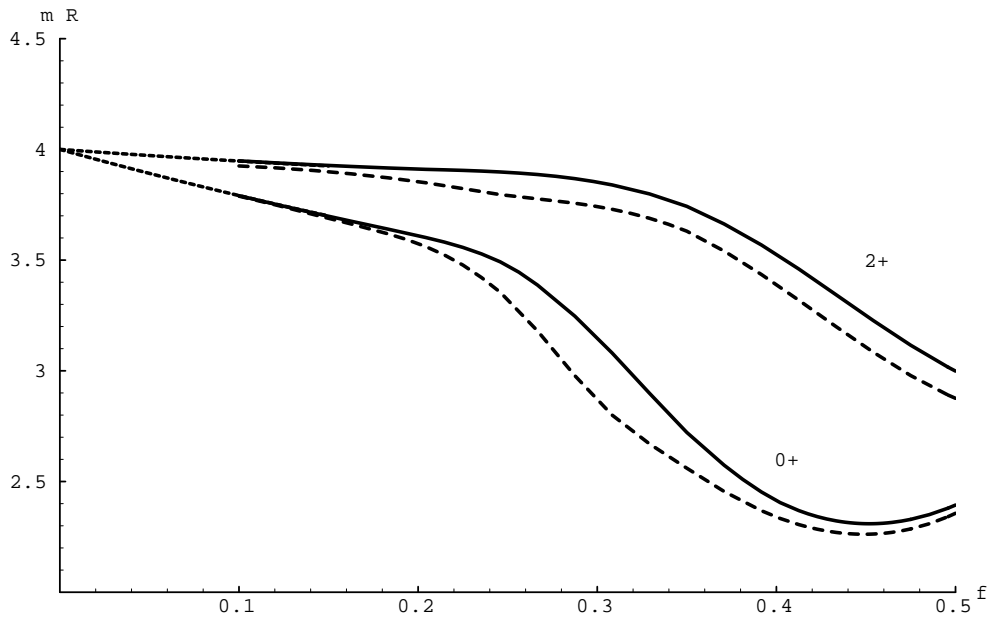


Figure 4: Glueball masses for $\beta = 0$ as a function of the coupling constant. The drawn curves are the masses of the first scalar (0^+) and tensor (2^+) glueball. The dashed lines denote the lower bounds, the dotted lines the perturbative results.

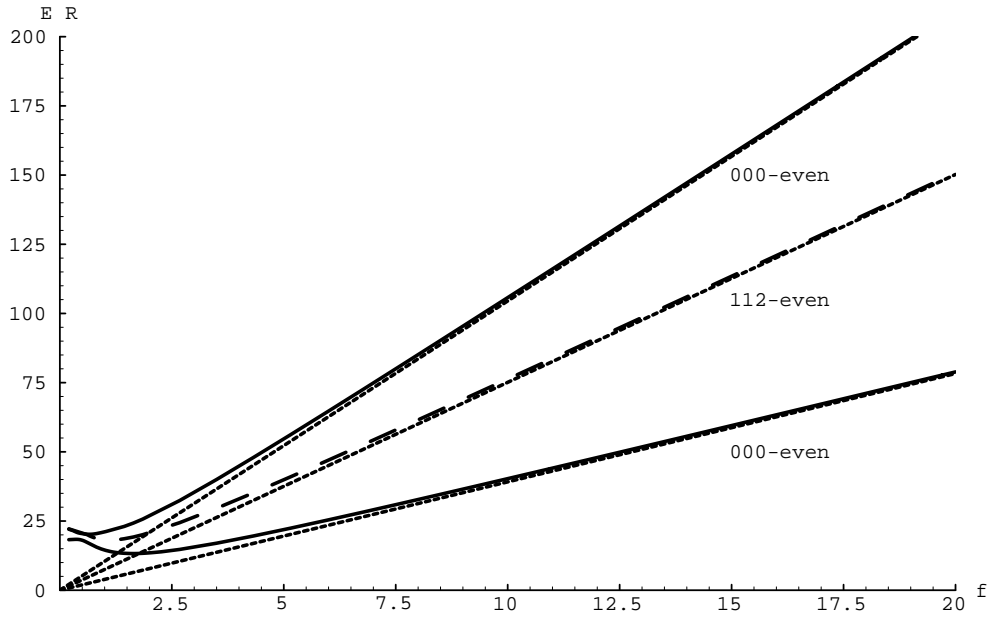


Figure 5: Strong coupling limit, $\beta = 0$: the drawn and dashed lines are the variational results for the lowest levels in the sectors 000-even and 112-even respectively. The dotted lines represent the analytic strong coupling limit.

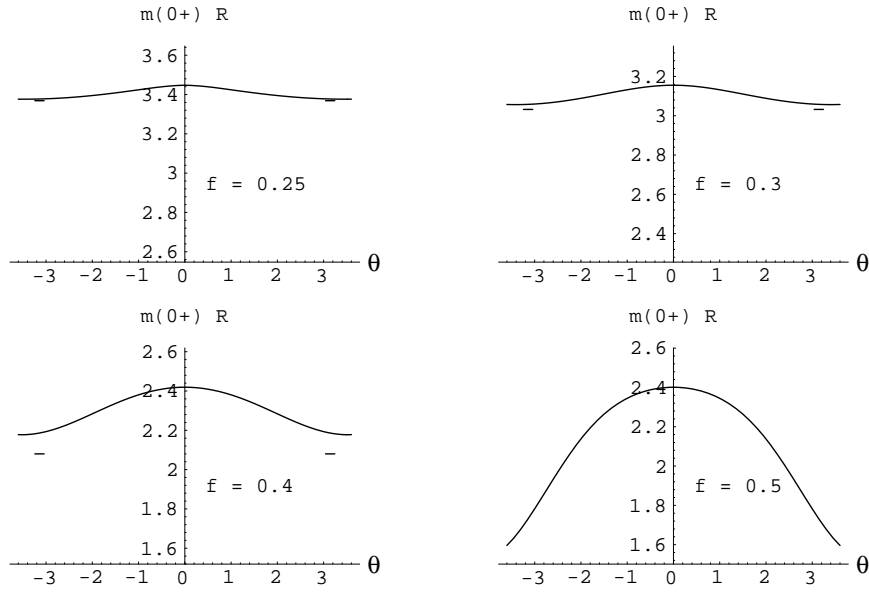


Figure 6: Scalar glueball mass at $f = 0.25$, $f = 0.3$, $f = 0.4$ and $f = 0.5$ as a function of θ . The dashes at $\theta = \pm 3$ denote the variational result with exact implementation of the boundary conditions. Note that the vertical range in these four plots is the same.

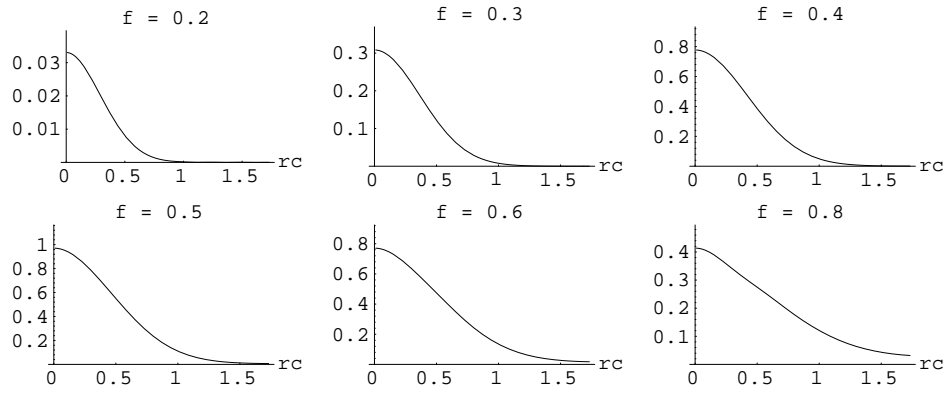


Figure 7: The wave function $j(r_c; r_d) / j(r_c^4, r_d^4)$ plotted at $r_d = \sqrt[4]{3}$ for the ground state in the sector 000-even.

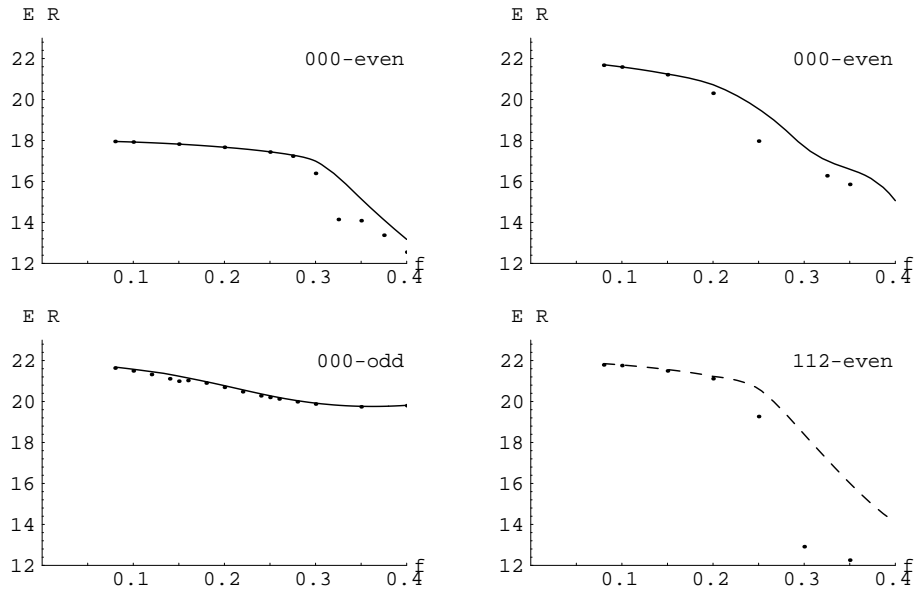
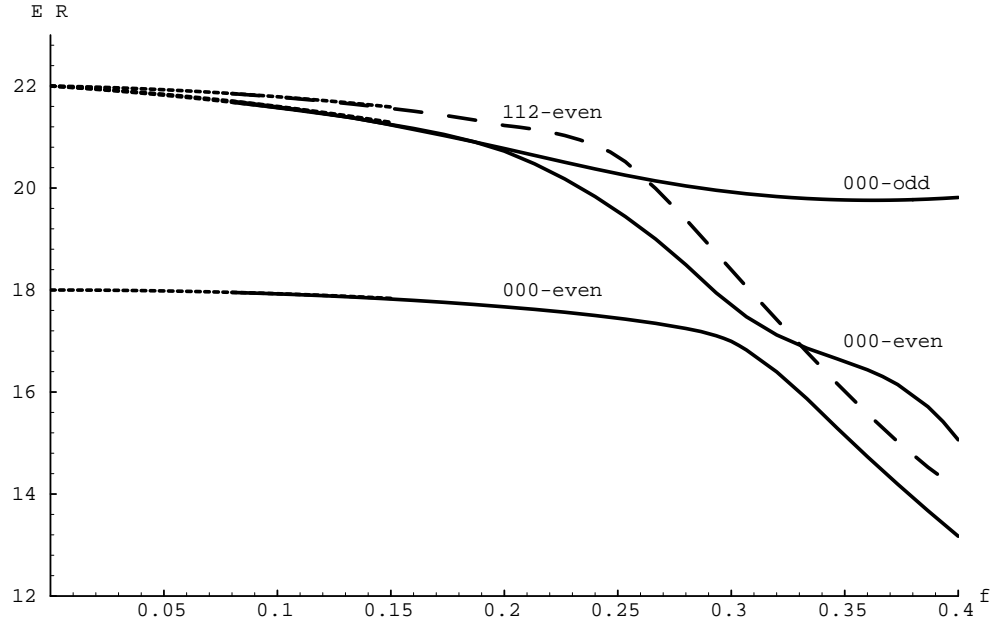


Figure 8: One-bop results. Lowest energy levels for $\epsilon = 0$. Drawn curves correspond to levels in the $(0;0;0)$ sector. The dashed curve denotes the ground level in the $(1;1;2)$ -even sector, the short-dashed curves are the perturbative expansions. The four small plots also show the lower bounds (individual dots) as obtained by Temple's inequality.

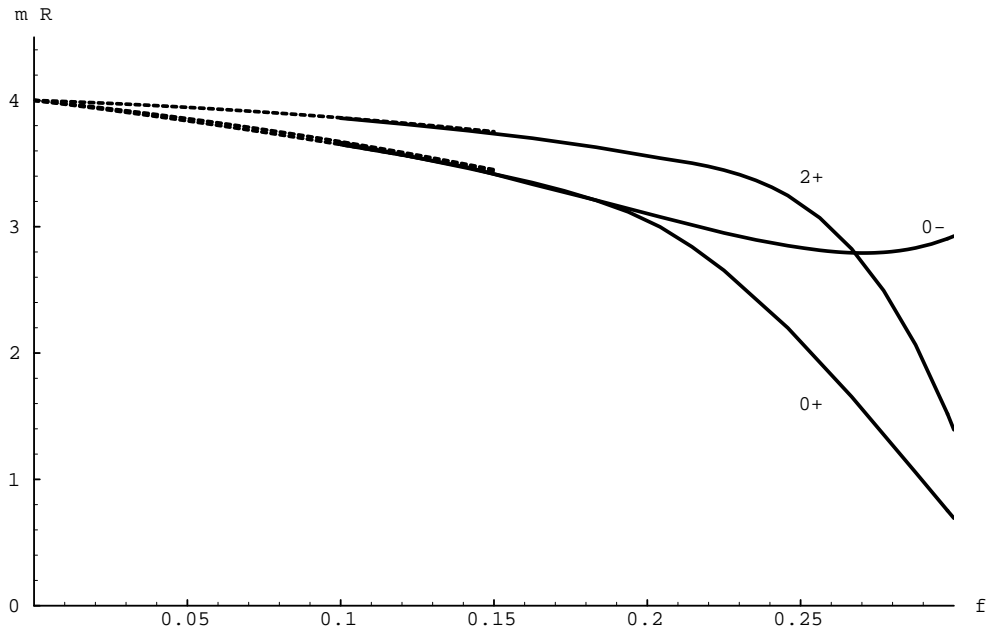


Figure 9: One-loop results. Glueball masses for $\beta = 0$ as a function of the coupling constant. The drawn curves are the masses of the various scalar and tensor glueballs. The dotted lines denote the perturbative results.

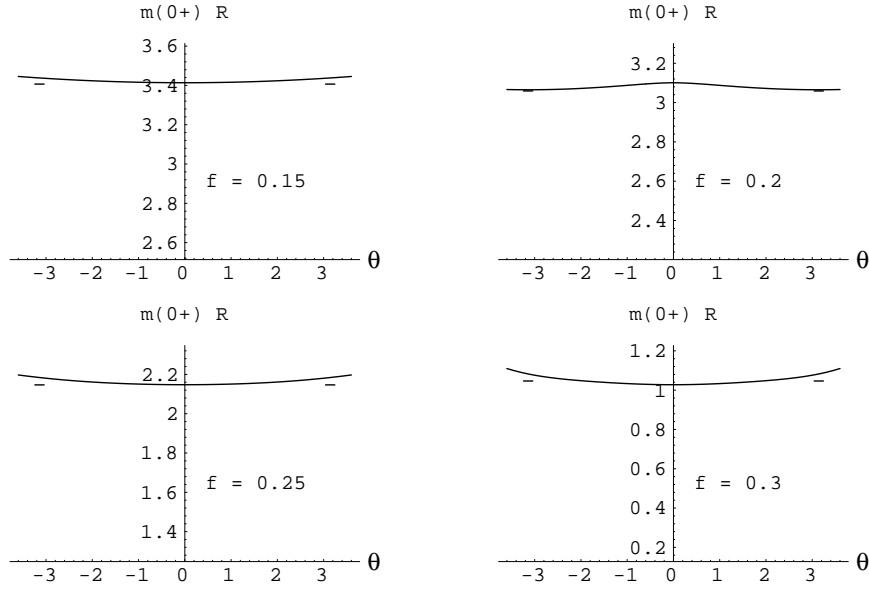


Figure 10: One-loop results. Scalar glueball mass at $f = 0.15$, $f = 0.2$, $f = 0.25$ and $f = 0.3$ as a function of θ . The dashes at $\theta = \pm 3$ denote the variational result with exact implementation of the boundary conditions. The vertical range of the plots is the same as in fig. 6.

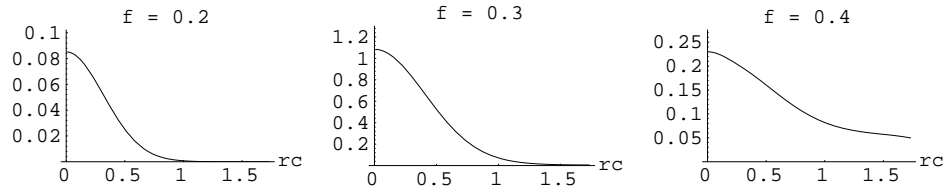


Figure 11: One-loop results. The wave function $\psi(r_c; r_d) / \sqrt{r_c^4 r_d^4}$ plotted at $r_d = \sqrt[3]{p}$ for the ground state in the sector 000-even.

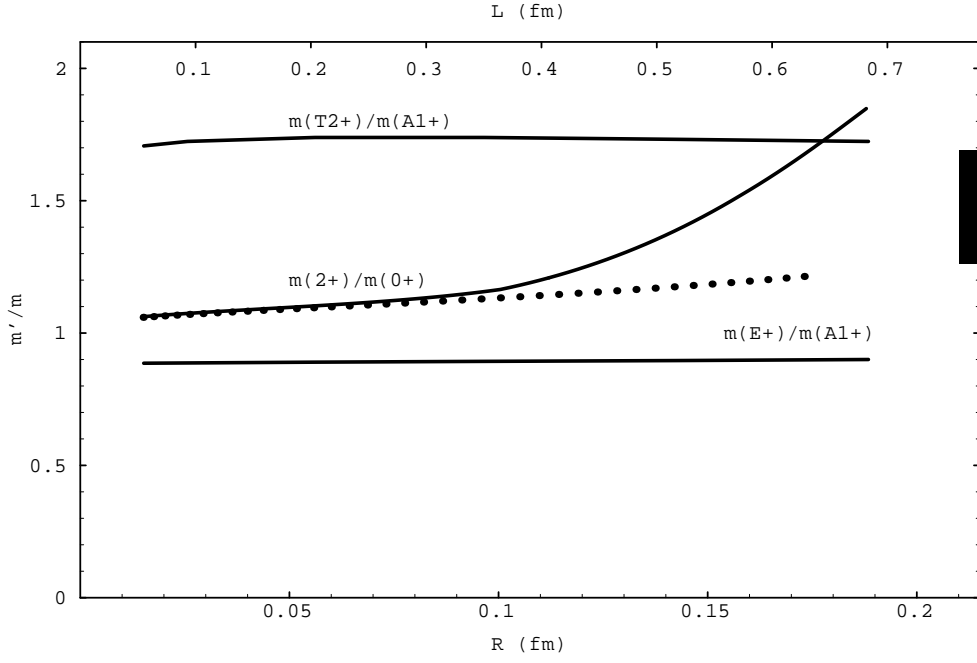


Figure 12: Comparison of the tensor to scalar mass ratio m_{2+}/m_{0+} as obtained on the three-sphere to the relevant ratios on the torus. The dotted line denotes the perturbative expansion, the bar on the right indicates the range of lattice Monte Carlo values at $L = 1$ to $L = 1.5 \text{ fm}$.